# Paired benthic foraminiferal Cd/Ca and Zn/Ca evidence for a greatly increased presence of Southern Ocean Water in the glacial North Atlantic

Thomas M. Marchitto Jr.
Lamont-Doherty Earth Observatory of Columbia University, Palisades, New York, USA

Delia W. Oppo and William B. Curry
Woods Hole Oceanographic Institution, Woods Hole, Massachusetts, USA

Received 13 October 2000; revised 2 April 2002; accepted 2 April 2002; published 15 August 2002.

[1] Benthic foraminiferal $\delta^{13}C$ and Cd/Ca studies suggest that deep Atlantic circulation during the Last Glacial Maximum was very different from today, with high-nutrient (low $\delta^{13}C$, high Cd) deep Southern Ocean Water (SOW) penetrating far into the North Atlantic. However, if some glacial $\delta^{13}C$ values are biased by productivity artifacts and/or air-sea exchange processes, then the existing $\delta^{13}C$ data may be consistent with the continual dominance of North Atlantic Deep Water (NADW). *Cibicidoides wuellerstorfi* Cd/Ca results presented here indicate that the glacial North Atlantic was strongly enriched in dissolved Cd below ~2500 m depth. If NADW formation was still vigorous relative to SOW formation, these data could be explained by either increased preformed nutrient levels in the high-latitude North Atlantic or by increased organic matter remineralization within lower NADW. High glacial Zn/Ca values in the same samples, however, are best explained by a substantially increased mixing with Zn-rich SOW. The cause was most likely a partial replacement of NADW by less dense Glacial North Atlantic Intermediate Water. This reorganization also lowered deep North Atlantic $CO_3^{2-}$ concentrations by perhaps 10 to 15 $\mu mol\ kg^{-1}$. *INDEX TERMS:* 4267 Oceanography: General: Paleoceanography; 4808 Oceanography: Biological and Chemical: Chemical tracers; 4825 Oceanography: Biological and Chemical: Geochemistry; 4875 Oceanography: Biological and Chemical: Trace elements; *KEYWORDS:* North Atlantic, LGM, cadmium, zinc, deep circulation

## 1. Introduction

[2] It has long been suggested that the formation of North Atlantic Deep Water (NADW) was curtailed during glacial periods [e.g., *Weyl*, 1968; *Newell*, 1974; *Duplessy et al.*, 1975]. *Curry and Lohmann* [1982] used benthic foraminifera to reconstruct a Last Glacial Maximum (LGM) bathymetric profile of $\delta^{13}C$ in the Vema Channel (western South Atlantic). They argued that their data indicated a shoaling of the boundary between northern and southern source deep waters, and speculated that this geometry could have resulted from a reduction or cessation of NADW production. *Boyle and Keigwin* [1982] showed that deep North Atlantic benthic foraminiferal Cd/Ca ratios, and thus seawater dissolved Cd concentrations, were higher during glacial periods. This suggested that the flux of nutrient-depleted NADW was indeed reduced relative to that of nutrient-rich southern source waters, though never completely ceased since Cd/Ca values remained lower than in the modern deep Pacific. Together these studies implied that deep Southern Ocean Water (SOW, equivalent to Antarctic Bottom Water (AABW) and/or Circumpolar Deep Water (CPDW)) was able to penetrate farther northward into the Atlantic during the LGM.


0883-8305/02/2000PA000598$12.00

[3] As spatial data coverage within the Atlantic increased, a more detailed picture of inferred LGM circulation emerged. Increased $\delta^{13}C$ and low Cd/Ca values in intermediate depth waters (above ~2000 m) signaled the presence of a nutrient-depleted water mass [*Oppo and Fairbanks*, 1987; *Boyle and Keigwin*, 1987]. *Boyle and Keigwin* [1987] argued that surface conditions in the glacial North Atlantic (colder but less saline) favored the production of intermediate waters rather than NADW. The extent of this water mass, dubbed Glacial North Atlantic Intermediate Water (GNAIW), was mapped in some detail by *Duplessy et al.* [1988] using $\delta^{13}C$. Additional $\delta^{13}C$ studies have further refined this view [e.g., *Oppo and Lehman*, 1993; *Sarnthein et al.*, 1994]. LGM Cd/Ca data agree with $\delta^{13}C$ on a gross scale, but differ in two important ways [*Boyle*, 1992; *Boyle and Rosenthal*, 1996]. First, $\delta^{13}C$ implies that North Atlantic intermediate waters were greatly depleted in nutrients relative to today, while Cd/Ca suggests a much smaller decrease; the main Cd/Ca change appears to be limited to deeper waters (note, however, that intermediate-depth Cd/Ca and $\delta^{13}C$ do imply similar nutrient depletions in some regions, such as the Bahama Banks [*Marchitto et al.*, 1998]). Second, $\delta^{13}C$ implies that Antarctic deep waters were greatly enriched in nutrients relative to today, while Cd/Ca again suggests little change. *Boyle and Rosenthal* [1996] suggested that the latter discrepancy is mainly due to a $\delta^{13}C$ artifact that occurs beneath regions of high surface water productivity

[*Mackensen et al.*, 1993]. A third paleonutrient tracer, benthic foraminiferal Ba/Ca, supports the existence of GNAIW and reduction of NADW, but suggests no contrast between the deep Atlantic and Pacific during the LGM [*Lea and Boyle*, 1990]. Deep Atlantic Ba may have become decoupled from Cd and $\delta^{13}C$ because of an increase in barite regeneration at the seafloor associated with increased productivity [*Lea and Boyle*, 1990; *Martin and Lea*, 1998].

[4] The hypothesis of NADW replacement by GNAIW and SOW assumes that surface ocean (''preformed'') nutrient levels in the glacial North Atlantic were not significantly different than today. *Mix and Fairbanks* [1985] noted the similarity between planktonic and benthic $\delta^{13}C$ records in the North Atlantic, and proposed that at least some of the glacial $\delta^{13}C$ depletion in the deep Atlantic could be explained by lower preformed values due to higher initial nutrient contents. They further speculated that if glacial NADW formed beneath sea and shelf ice, then the combination of increased preformed nutrients and reduced air-sea isotopic exchange might explain the entire deep Atlantic $\delta^{13}C$ decrease. The planktonic foraminifer used by *Mix and Fairbanks* [1985] (*Neogloboquadrina pachyderma* (s.)) has since been shown to be a poor recorder of seawater $\delta^{13}C$, however [*Keigwin and Boyle*, 1989; *Kohfeld et al.*, 2000]. Nevertheless, remaining uncertainties in the end-member compositions of glacial northern and southern source waters make volumetric deep water reconstructions somewhat ambiguous [*LeGrand and Wunsch*, 1995]. Vigorous NADW flow could explain the sedimentary $^{231}Pa/^{230}Th$ observations of *Yu et al.* [1996], though vigorous GNAIW flow could do the same.

[5] The idea of NADW's persistent dominance over SOW during the LGM was revived by *Matsumoto and Lynch-Stieglitz* [1999]. They proposed that many Southern Ocean benthic $\delta^{13}C$ data are affected by *Mackensen et al.*'s [1993] productivity artifact, and argued that the ''true'' LGM Southern Ocean value (2500–4000 m) must be close to −0.2‰. Thus LGM deep ocean $\delta^{13}C$ decreased from north to south in the Atlantic and from south to north in the Pacific, as it does today. In addition, the LGM ''whole deep ocean'' gradient (∼1.1‰) was the same as today, although the Southern Ocean appears to have been slightly closer to Pacific values. The authors concluded that a significant amount of NADW must have formed during the LGM. They further noted that the glacial $\delta^{13}C$ data could be consistent with a circulation pattern very similar to today, without an increased northward migration of SOW. They did not rule out the presence of GNAIW, but proposed that the vertical gradient in glacial $\delta^{13}C$ was mainly caused by differences in preformed values, largely due to latitudinal gradients in North Atlantic air-sea exchange [*Lynch-Stieglitz and Fairbanks*, 1994]. Although *Matsumoto and Lynch-Stieglitz*'s [1999] observations are also consistent with a mixing between reduced-volume NADW and northward-penetrating SOW, their proposed circulation scheme cannot be ruled out using $\delta^{13}C$ alone.

[6] Under a scenario of Holocene-like NADW flux, deep North Atlantic LGM Cd/Ca data [*Boyle*, 1992] require that either high-latitude North Atlantic preformed nutrients were higher, or that lower NADW collected more remineralized nutrients over a given distance than it does today. An increase in preformed Cd is in apparent contradiction with planktonic (*N. pachyderma*) Cd/Ca data [*Keigwin and Boyle*, 1989]. However, *Rickaby and Elderfield* [1999] have suggested that Cd incorporation into the planktonic foraminifer *Globigerinoides bulloides* increases strongly with temperature. If applicable to *N. pachyderma*, *Keigwin and Boyle*'s [1989] glacial North Atlantic data may underestimate surface water Cd concentrations. An increase in nutrient accumulation independent of mixing (i.e., ''aging''), which could occur by increased particulate rain rates or by more sluggish circulation, is difficult to rule out using published data. It would only require that GNAIW formation was much more rapid than the southward progression of deeper waters, a situation that is supported by sedimentological current speed evidence [e.g., *Ledbetter and Balsam*, 1985; *Haskell et al.*, 1991; *McCave et al.*, 1995]. Such a reduction in lower NADW flow without an increased admixture of SOW would presumably require a corresponding decrease in SOW formation.

[7] We propose that the ambiguity surrounding SOW penetration into the North Atlantic may be resolved using benthic foraminiferal Zn/Ca. In the modern ocean, both dissolved Cd and dissolved Zn are completely removed from most surface waters, but Zn has a deeper regeneration cycle [e.g., *Boyle et al.*, 1976; *Bruland et al.*, 1978; *Bruland*, 1980]. While AABW-like Cd concentrations (estimated from P) are found in intermediate waters as far north as 15°N in the western North Atlantic, AABW-like Zn concentrations (estimated from Si) are limited to deep Southern Ocean waters (Figure 1). Since intermediate waters are the main source of nutrients to the North Atlantic surface, any glacial increase in preformed Cd would be accompanied by a comparatively small increase in preformed Zn. Similarly, the low Zn:Cd ratio of these upper waters would limit the biological export of Zn (relative to Cd) to deeper waters. Thus the only way to produce high Zn:Cd ratios in the deep North Atlantic would be by mixing with SOW. Ba is also preferentially concentrated in deep SOW because of a deep regeneration cycle, but to a lesser degree than Zn since Ba is not as efficiently removed from surface waters [*Chan et al.*, 1977]. *Marchitto et al.* [2000] have shown that Zn/Ca ratios in the benthic foraminifera *Cibicidoides wuellerstorfi* and *Uvigerina* reflect bottom water dissolved Zn concentrations and, like Cd/Ca and Ba/Ca [*McCorkle et al.*, 1995; *Elderfield et al.*, 1996], bottom water saturation state with respect to calcite ($\Delta CO_3^{2-}$).

## 2. Study Area and Previous Work

[8] The nine sediment cores used in this study are confined to the North Atlantic above 40°N and span a depth range of 1326 to 3427 m (Figure 2 and Table 1; for simplicity, no correction for lowered sea level will be made to the LGM depths). Four of the cores, including the three deepest, are from the flanks of the Mid-Atlantic Ridge between ∼42°N and 44°N. The other five cores are from the northeast North Atlantic between ∼55°N and

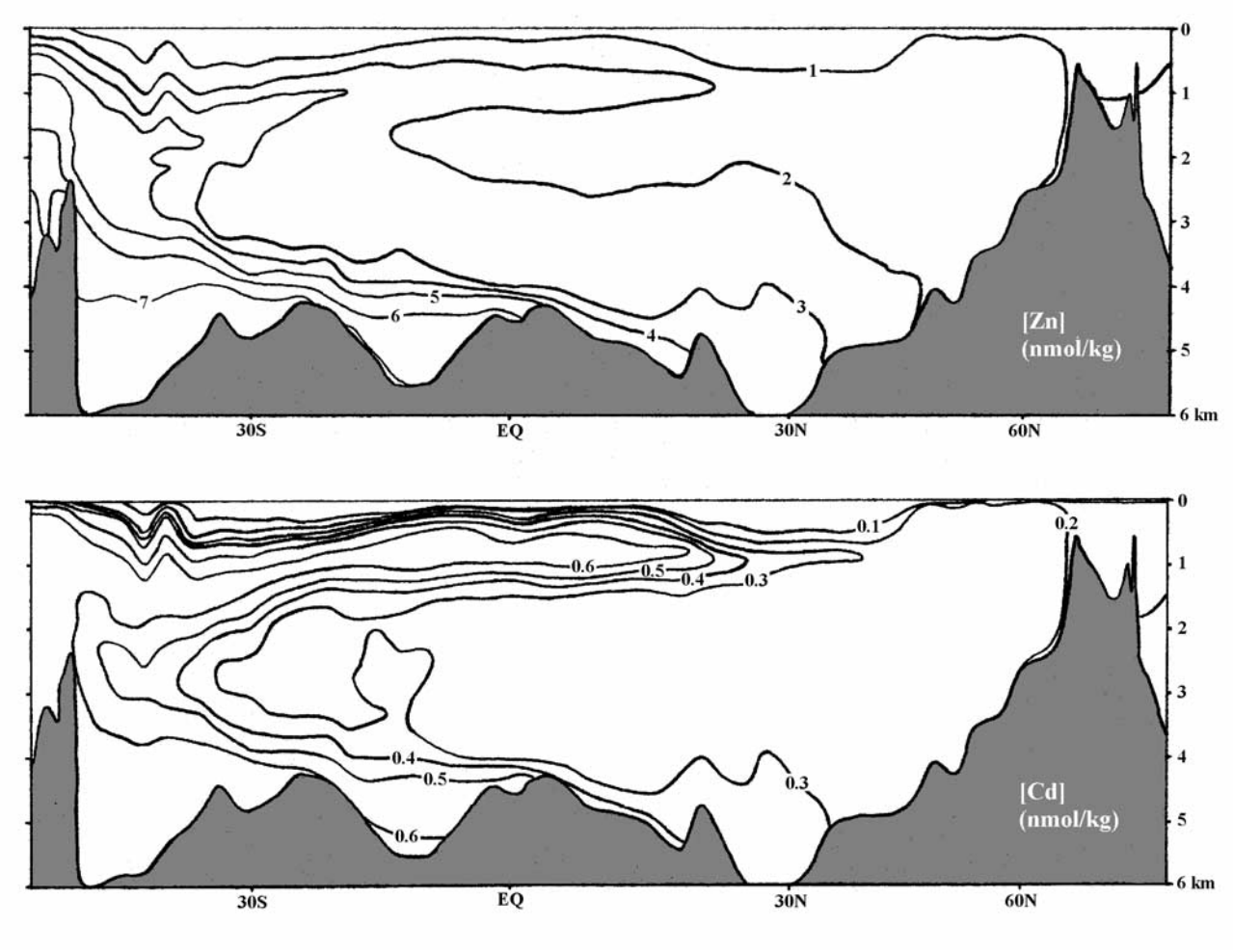


**Figure 1.** (top) Inferred modern dissolved Zn concentrations in the western Atlantic Ocean, calculated from GEOSECS dissolved Si measurements [*Bainbridge*, 1981] using the linear deep water relationship of *Marchitto et al.* [2000], except that the trend is forced through the origin at very low concentrations (i.e., the 1 nmol $kg^{-1}$ contour is drawn at [Si] = 8 μmol $kg^{-1}$ instead of [Si] = 4 μmol $kg^{-1}$). (bottom) Inferred modern dissolved Cd concentrations calculated from GEOSECS dissolved P measurements using the two-part linear relationship of *Boyle* [1988].

61°N. Today all of the sites are bathed by nearly pure NADW, with potential temperatures of ~2–4°C and salinities of ~34.9–35.0‰ (we use "pure NADW" as a generic term to describe deep waters originating in the north, before any significant mixing with deep or intermediate waters from the south; it is close to, but not necessarily identical to, *Broecker and Peng*'s [1982] Northern Component Water (NCW)). There is a slight increase in dissolved nutrients between the northeastern and Mid-Atlantic Ridge regions, with P increasing by roughly 0.1 μmol $kg^{-1}$ (~0.02 nmol $kg^{-1}$ Cd) and Si increasing by roughly 3 μmol $kg^{-1}$ (~0.2 nmol $kg^{-1}$ Zn) [*Bainbridge*, 1981]. These gradients are small compared to the scatter typical of foraminiferal data, and the nine cores will be treated together in this study. $\Delta CO_3^{2-}$ estimates recalculated from nearest GEOSECS data [*Bainbridge*, 1981] following the recommendations of *United Nations Educational, Scientific, and Cultural Organization* (*UNESCO*) [1987] range from ~23 to 45 μmol $kg^{-1}$. Although Zn partition coefficients begin to decrease below ~25 μmol $kg^{-1}$ $\Delta CO_3^{2-}$ [*Marchitto et al.*, 2000], no correction will be made to the Holocene Zn/Ca data.

[9] *C. wuellerstorfi* $\delta^{13}C$ has been previously measured in the late Holocene and LGM sections of each core [*Boyle and Keigwin*, 1982, 1985/1986, 1987; *Boyle*, 1992; *Oppo and Lehman*, 1993, 1995; *Curry et al.*, 1999; *McManus et al.*, 1999] (Figure 3 and Table 1). Holocene means are relatively uniform with depth (1.13 ± 0.10‰), as expected from the water column measurements of *Kroopnick* [1985]. LGM means are enriched (relative to the Holocene) by up to 0.38‰ above ~2000 m and depleted by up to 0.63‰ below this depth. The exception is CHN82-15PC at 2153 m and 43°N, which has a glacial enrichment of 0.25‰, though the Holocene value in this core is poorly constrained.

[10] Benthic foraminiferal (*C. wuellerstorfi*, *C. kullenbergi*, and *Uvigerina*) Cd/Ca has also been previously measured in

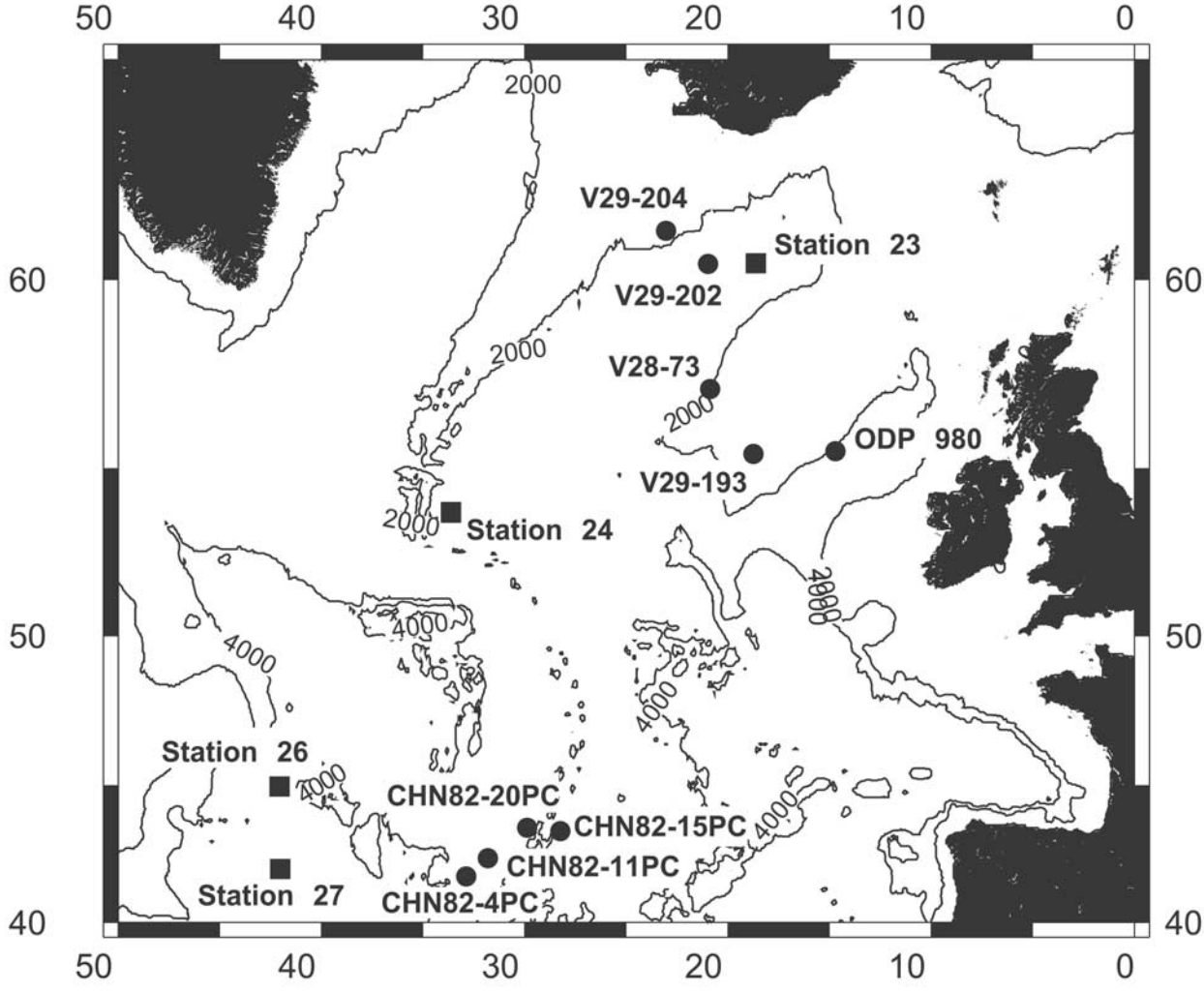


**Figure 2.** Locations of sediment cores (circles) and GEOSECS stations (squares) used in this study. See Table 1 for core coordinates and water depths.

the four CHN82 cores [*Boyle and Keigwin*, 1982, 1985/1986, 1987; *Boyle*, 1992]. Below 3000 m, LGM means are higher than Holocene means by up to 0.05 μmol mol$^{-1}$, while the shallower core (2153 m) shows a glacial depletion of 0.01 μmol mol$^{-1}$. This general pattern is consistent with the $\delta^{13}C$ results. Since our new measurements give us the opportunity to compare Cd/Ca and Zn/Ca in the same samples, we will not incorporate the older Cd/Ca data in

**Table 1.** Core Locations and Previously Published *C. wuellerstorfi* $\delta^{13}C$ Data

| Core | Location | Depth, m | Holocene Depth,[a] cm | Holocene $\delta^{13}C$,[b] ‰ | LGM Depth,[a] cm | LGM $\delta^{13}C$,[b] ‰ | Reference |
|---|---|---|---|---|---|---|---|
| V29-193 | 55.40°N, 18.73°W | 1326 | 15 | 1.12 | 55–64.5 | 1.50 ± 0.12 | *Oppo and Lehman* [1993] |
| V29-204 | 61.18°N, 23.02°W | 1849 | 5–36 | 1.24 ± 0.07 | 201–235 | 1.37 ± 0.09 | *Curry et al.* [1999] |
| V28-73 | 57.18°N, 20.87°W | 2063 | 3.5–15 | 1.17 ± 0.14 | 43–64 | 1.16 ± 0.09 | *Oppo and Lehman* [1993] |
| CHN82-15PC | 43.37°N, 28.23°W | 2153 | 2–6 | 0.96 ± 0.46 | 29–33 | 1.21 ± 0.05 | *Boyle and Keigwin* [1987] |
| ODP 980[c] | 55.48°N, 14.70°W | 2168 | 0–24 | 1.04 ± 0.07 | 402–442 | 0.82 ± 0.03 | *McManus et al.* [1999] |
| V29-202 | 60.38°N, 20.97°W | 2658 | 4–21, 31–35 | 1.06 ± 0.18 | 100–114 | 0.45 ± 0.05 | *Oppo and Lehman* [1995] |
| CHN82-20PG/C[d] | 43.50°N, 29.87°W | 3070 | 3.5–15 | 1.30 ± 0.14 | 79–89 | 0.76 ± 0.12 | *Keigwin and Lehman* [1994] |
| CHN82-11PC | 42.38°N, 31.80°W | 3209 | 11–20 | 1.17 ± 0.34 | 70–80 | 0.66 ± 0.06 | *Boyle and Keigwin* [1982][e] |
| CHN82-4PC | 41.72°N, 32.85°W | 3427 | 1–4 | 1.11 | 56–65 | 0.48 ± 0.06 | *Boyle and Keigwin* [1985/1986] |

[a] Sample depths refer to $\delta^{13}C$ data only; our trace metal sample depths are listed in Table 2.
[b] The $\delta^{13}C$ errors are ±1σ on means of 2 to 14 measurements.
[c] Sample depths are composite; actual sample IDs are 980B-1H-01, 0–24 cm (Holocene), and 980C-2H-01, 44–86 cm (LGM).
[d] Holocene depths are from the pilot gravity core and LGM depths are from the piston core (not composite).
[e] Data from *Boyle and Keigwin* [1982] are here corrected following the recommendations of *Craig* [1957] (L. Keigwin, personal communication, 2000).

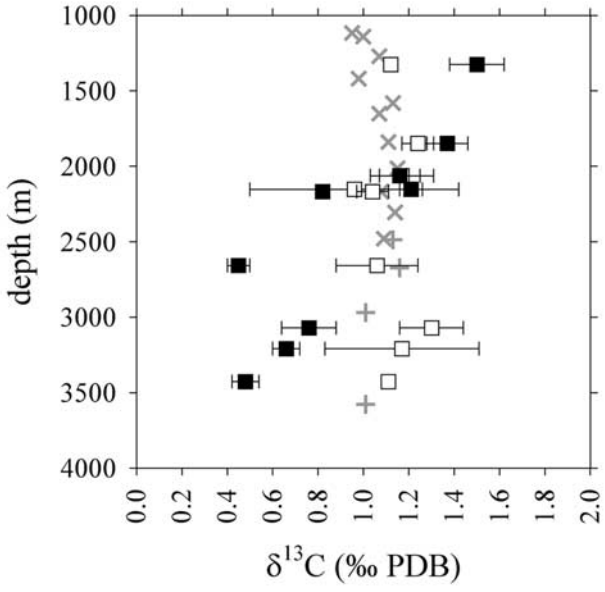


**Figure 3.** Previously published *C. wuellerstorfi* $\delta^{13}C$ data from the late Holocene (open squares) and LGM (solid squares) sections of the nine cores used in this study (see Table 1 for references). Error bars are $\pm 1\sigma$. Also shown are modern water column measurements from GEOSECS stations 23 (60°N, 19°W; crosses) and 26 (45°N, 42°W; pluses) [*Kroopnick*, 1985].

our calculations. A brief comparison of the two Cd/Ca data sets is included in the results section.

## 3. Materials and Methods

[11] Late Holocene and LGM intervals of each sediment core were identified using previously generated stable isotope data [*Boyle and Keigwin*, 1982, 1985/1986, 1987; *Boyle*, 1992; *Oppo and Lehman*, 1993, 1995; *Curry et al.*, 1999; *McManus et al.*, 1999] (Figure 4). Zn, Cd, and Mn concentrations were measured in shells of the benthic foraminifera *C. wuellerstorfi*, *C. kullenbergi*, *C. pachyderma*, *C. rugosus*, and *Uvigerina* spp. Each sample consisted of ~5 to 15 individuals (>250 μm), and was cleaned following the methods of *Boyle and Keigwin* [1985/1986] as modified by *Boyle and Rosenthal* [1996]. Samples were generally kept covered when outside of laminar flow benches to minimize the risk of dust-borne laboratory contamination, which has historically been a major obstacle to Zn work [*Bruland et al.*, 1978]. Zn, Cd, and Mn were measured sequentially by graphite furnace atomic absorption spectrophotometry (AAS) and Ca was measured by flame AAS, all on a Hitachi Z-8200. Analytical precision, based on frequent analyses of three consistency standards, is ±2–3% for Zn, ±3–6% for Cd, ±8–9% for Mn, and ±1% for Ca.

## 4. Results and Discussion

### 4.1. Cd/Ca Profiles

[12] Holocene and LGM *C. wuellerstorfi* Cd/Ca values measured in each core are shown in Figure 5a and listed (along with *C. kullenbergi*, *C. pachyderma*, *C. rugosus*, and *Uvigerina* data) in Table 2. Results from all five taxa agree with previously published data from above 40°N in the North Atlantic [*Boyle and Keigwin*, 1982, 1985/1986, 1987; *Boyle*, 1992; *Bertram et al.*, 1995; *Rickaby et al.*, 2000] in that LGM values are lower than Holocene above ~2500 m and higher than Holocene below this depth. The only exception is core V29-204 at 1849 m, whose Holocene *C. wuellerstorfi* values are slightly lower than its LGM. All but five Mn/Ca measurements are below 100 μmol $mol^{-1}$ (Table 2), suggesting that Mn-carbonate overgrowths are not a major source of contamination.

[13] Our *C. wuellerstorfi* Cd/Ca values are significantly higher than coexisting *C. kullenbergi* and *Uvigerina* values in the three deepest cores. Such large offsets (0.02 to 0.05 μmol $mol^{-1}$) are not unusual in deep sea cores and may reflect, in part, the mixing together of noncontemporaneous individuals [*Boyle*, 1992, 1995]. Boyle reported *C. wuellerstorfi* data from only one of these cores, CHN82-20 (3070 m) [*Boyle and Keigwin*, 1985/1986]. He found no consistent offset between *C. wuellerstorfi* and the other two taxa, but there is a large amount of variability in the data. A species-by-species comparison of our data with Boyle's does not suggest any significant analytical offset, nor does an interlaboratory standard calibration (our unpublished data). Heinrich events 1 and 2 could be mixed into some of the glacial data, though this is not the case for CHN82-20, the only one of the deep cores where Heinrich event 1 has been clearly identified [*Keigwin and Lehman*, 1994]. Glacial values above 0.15 μmol $mol^{-1}$ occur elsewhere in the North Atlantic, such as in Bermuda Rise core EN120-GGC1 (4450 m) which reached 0.22 μmol $mol^{-1}$ [*Boyle and Keigwin*, 1987].

[14] The ensuing discussion will focus on *C. wuellerstorfi* for three reasons. First, it is the only species present in both Holocene and LGM sections from all water depths (the exception being the Holocene of ODP 980, where none of the four taxa were available). Second, *C. kullenbergi* and *C. pachyderma* either have very high and unconstrained Zn partition coefficients or else are prone to Zn contamination (Table 2), making direct comparisons to other species impossible. Finally, we feel that *Uvigerina* is likely to be a less accurate recorder of bottom water conditions because of its shallow infaunal habitat [*Zahn et al.*, 1986; *McCorkle et al*, 1997] (whereas *C. wuellerstorfi* has been observed to prefer an elevated epifaunal position [*Lutze and Thiel*, 1989]). For example, although bottom water $\Delta CO_3^{2-}$ is probably an issue for LGM Zn/Ca only, pore water $\Delta CO_3^{2-}$ might become low enough in the top 1 cm [e.g., *Martin and Sayles*, 1996] to affect *Uvigerina* Cd/Ca.

[15] Holocene and LGM profiles of inferred seawater Cd concentration ($Cd_W$), converted from *C. wuellerstorfi* Cd/Ca using the depth-dependent partition coefficients of *Boyle* [1992], are shown in Figure 5b. Most of the Holocene data are slightly higher than predicted from modern dissolved P estimates [*Bainbridge*, 1981]. Since these samples are not from truly modern sediments, it is possible that they record earlier Holocene times when $Cd_W$ could have been somewhat higher. Two of the shallow Holocene data (V29-193 at 1326 m and V28-73 at 2063 m) are

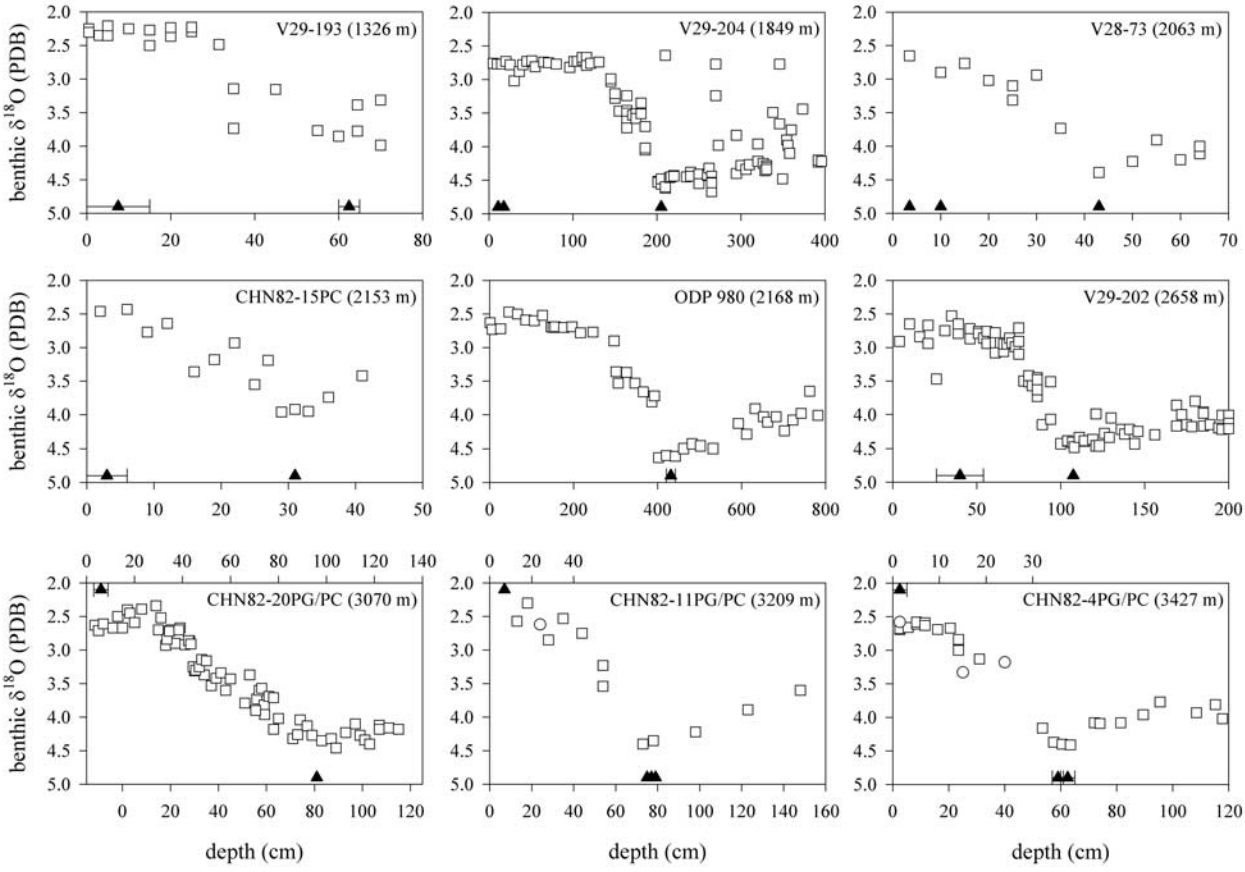


**Figure 4.** Previously published benthic $\delta^{18}O$ stratigraphies (squares, mostly *C. wuellerstorfi* with some *C. kullenbergi*) for the nine cores used in this study (see Table 1 for references). Triangles show the depths of our trace metal data. The three deepest cores are composites of piston cores (lower horizontal axes) and pilot gravity cores (upper horizontal axes). Trace metal samples taken from the gravity cores are shown adjacent to the upper axes. For the two deepest cores we have used our own $\delta^{18}O$ data (circles) to verify that the gravity cores are Holocene in age; the resulting splices are not intended to be precise.

much higher than expected, however, a problem noted by *Bertram et al.* [1995] in several cores from the same region (northeast North Atlantic above 50°N). They concluded that regional partition coefficients are elevated for some unspecified reason, but two of our other cores from this area (V29-202 and V29-204) do not share this pattern. We suggest that the tops of V28-73, V29-193, and some of *Bertram et al.*'s [1995] cores might be affected by sedimentary contamination. This problem may be prevalent in the northeast North Atlantic, but it is clearly not ubiquitous. LGM data from the cores with elevated Holocene values appear to agree well with other LGM data (Figure 5), implying that any contamination is probably limited to the upper sections of these cores.

[16] LGM $Cd_W$ data above ~2500 m are similar to modern predicted values, while deeper data are significantly enriched in Cd. This is essentially the same pattern observed by *Boyle* [1992], but with a greater deep enrichment. The deepest values (0.52–0.58 nmol $kg^{-1}$) are close to those observed in LGM *C. wuellerstorfi* from the low-latitude eastern North Atlantic below ~3500 m (0.52–0.54 nmol $kg^{-1}$) [*Boyle*, 1992; *Beveridge et al.*, 1995]. The difference between LGM and Holocene values increases with depth, from 0.07 nmol $kg^{-1}$ at 2658 m to 0.23 nmol $kg^{-1}$ at 3427 m. Differences from modern predicted values increase from ~0.17 to 0.33 nmol $kg^{-1}$.

### 4.2. Zn/Ca Profiles

[17] Holocene and LGM *C. wuellerstorfi* Zn/Ca measurements from each core are shown in Figure 5c and listed (with data from the other taxa) in Table 2. *C. wuellerstorfi* values are again significantly higher than coexisting *Uvigerina* specimens in the two deepest cores, and Holocene *C. kullenbergi* data are either contaminated or imply a partition coefficient close to 50. Five of the eight *C. wuellerstorfi* Holocene means are in excellent agreement with estimates based on modern dissolved Si concentrations [*Bainbridge*, 1981] using a partition coefficient ($D_{Zn}$) of 9 [*Marchitto et al.*, 2000]. The three Holocene values that are higher than predicted are from the same cores that were most elevated in Cd/Ca. Again, core V29-204 (1849 m) shows no Holocene elevation. LGM *C. wuellerstorfi* Zn/Ca values are similar to Holocene data above ~2500 m and enriched below this depth, in general agreement with the glacial $Cd_W$ pattern.

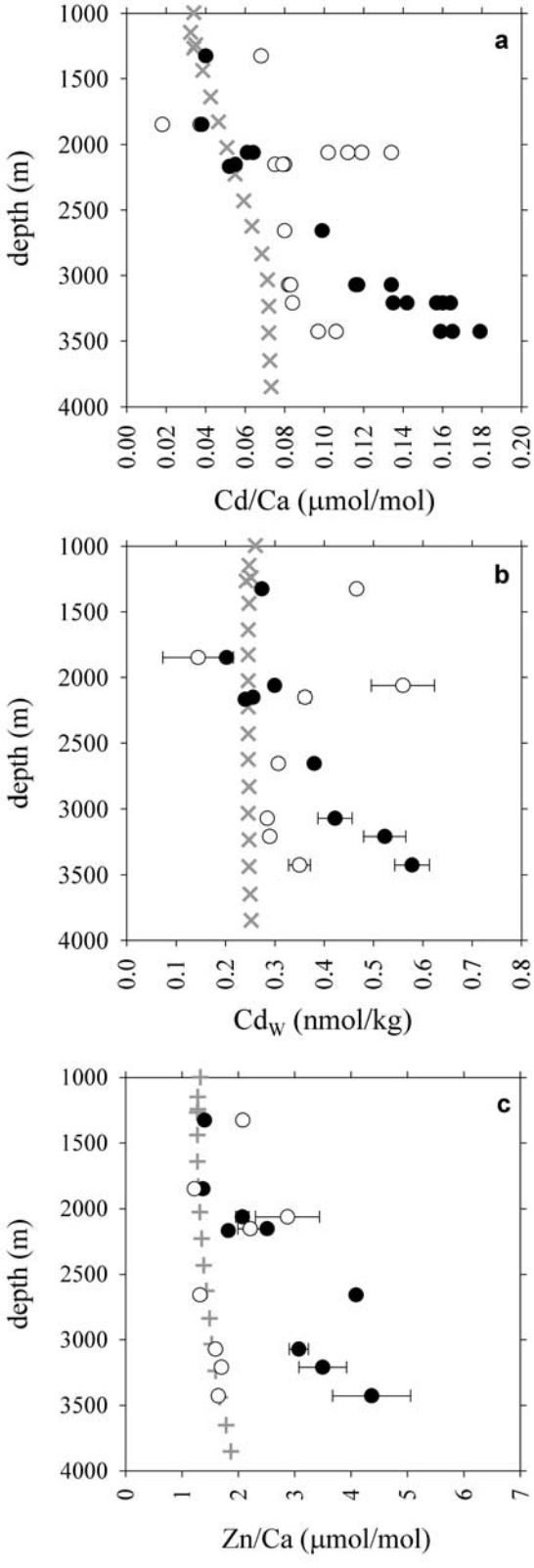


The deep LGM Zn/Ca values range from 3.1 to 4.4 μmol $mol^{-1}$, or about 1.5 to 2.7 μmol $mol^{-1}$ higher than today.

[18] To determine whether or not the deep glacial Zn/Ca enrichment requires a significant contribution from SOW, the LGM $Cd_W$ data from the four deepest cores will be modeled according to three scenarios: (1) increased preformed nutrient concentrations in the high-latitude North Atlantic; (2) greater addition of remineralized organic matter to lower NADW (aging); and (3) decreased relative flux of NADW and increased mixing with SOW. Each model will produce predicted Zn/Ca values, which will then be compared to the actual measurements. All calculations in the text will use the data from core CHN82-20 (3070 m) as an example; results from all four deepest cores are listed in Table 3. Note that two to three significant digits will be used for calculations, but we make no claim that the various parameters are known to such high precision.

### 4.3. Modern Circulation Model

[19] Before attempting to infer LGM deep circulation, it is necessary to adopt a simple nutrient model that works for the modern ocean. We assume that deep water nutrient concentrations change by two mechanisms: remineralization of biological rain (aging) and mixing with other water masses. These processes will be modeled using dissolved Cd and Zn; Cd is estimated from GEOSECS P measurements using the two-part linear relationship of *Boyle* [1988] and Zn is estimated from GEOSECS Si measurements using the linear relationship of *Marchitto et al.* [2000]. *Elderfield and Rickaby* [2000] recently suggested that the Cd:P relationship is better defined using curves that depend on a regionally varying Cd/P fractionation factor, α. We choose to retain *Boyle*'s [1988] equations for simplicity and consistency with previous paleoceanographic studies. Since we combine the Cd:P relationship with a rather crudely defined linear Zn:Si relationship, we feel that *Boyle*'s [1988] equations are adequate for our purposes. The two-part global Cd:P relationship is a reasonable approximation of *Elderfield and Rickaby*'s [2000] Atlantic curve ($\alpha = 2.5$) and is therefore a reasonable approximation of Cd:P remineralization within the Atlantic. It will be seen in a later section that this choice of equations has little impact on our results.

[20] The aging process within the North Atlantic can be examined by following modern P and Si from the region of

**Figure 5.** (opposite) (a) New Cd/Ca measurements on Holocene (open circles) and LGM (solid circles) *C. wuellerstorfi* from the North Atlantic. Also shown (crosses) are modern predictions based on dissolved P measurements at GEOSECS station 27 (42°N, 42°W) [*Bainbridge*, 1981], using the Cd:P relationship of *Boyle* [1988] and the depth-dependent partition coefficients of *Boyle* [1992]. (b) As in Figure 5a but averaged and converted to inferred seawater Cd concentrations ($Cd_W$) using the partition coefficients of *Boyle* [1992]. Error bars are ±1σ. (c) Mean Zn/Ca measured in the same North Atlantic *C. wuellerstorfi* samples as used for Cd/Ca. Pluses are modern predictions based on dissolved Si measurements at GEOSECS station 27 assuming a partition coefficient of 9 [*Marchitto et al.*, 2000].

**Table 2.** Trace Metal Data From this Study, Grouped by Species[a]

| Core | Sample Depth,[b] cm | [Ca], (m*M*) | Zn/Ca, μmol mol$^{-1}$ | Cd/Ca, μmol mol$^{-1}$ | Mn/Ca, μmol mol$^{-1}$ |
|---|---|---|---|---|---|
| | | *C. wuellerstorfi* | | | |
| V29-193 (1326 m) | 0–15 (H) | 28.60 | 2.08 | 0.068 | 50.0 |
| V29-193 (1326 m) | 60–65 (G) | 24.07 | 1.40 | 0.040 | 68.6 |
| V29-204 (1849 m) | 10–12 (H) | 7.56 | nm | 0.037 | 30.3 |
| V29-204 (1849 m) | 15–20 (H) | 4.69 | 1.22 | 0.018 | 66.9 |
| V29-204 (1849 m) | 205 (G) | 13.98 | 1.37 | 0.038 | 226.9 |
| V28-73 (2063 m) | 3–4 (H) | 15.03 | 3.62 | 0.102 | 44.9 |
| V28-73 (2063 m) | 3–4 (H) | 12.95 | 3.00 | 0.119 | 48.1 |
| V28-73 (2063 m) | 10 (H) | 8.77 | 2.38 | 0.134 | 34.8 |
| V28-73 (2063 m) | 10 (H) | 13.82 | 2.48 | 0.112 | 44.6 |
| V28-73 (2063 m) | 43 (G) | 22.33 | 2.15 | 0.064 | nm |
| V28-73 (2063 m) | 43 (G) | 21.45 | 1.99 | 0.061 | nm |
| CHN82-15PC (2153 m) | 0–6 (H) | 15.05 | 1.96 | 0.075 | 13.7 |
| CHN82-15PC (2153 m) | 0–6 (H) | 7.88 | 2.26 | 0.080 | 9.3 |
| CHN82-15PC (2153 m) | 0–6 (H) | 12.94 | **3.48** | **0.127** | 16.1 |
| CHN82-15PC (2153 m) | 0–6 (H) | 17.31 | 2.40 | 0.079 | 13.2 |
| CHN82-15PC (2153 m) | 31 (G) | 26.11 | 2.51 | 0.055 | 11.0 |
| ODP 980 (2168 m) | 421–442 (G)[c] | 10.15 | 1.82 | 0.052 | nm |
| V29-202 (2658 m) | 26–54 (H) | 23.89 | 1.32 | 0.080 | 170.8 |
| V29-202 (2658 m) | 107–108 (G) | 10.15 | 4.09 | 0.099 | 198.3 |
| CHN82-20PG (3070 m) | 3–9 (H) | 11.21 | 1.64 | 0.082 | 18.5 |
| CHN82-20PG (3070 m) | 3–9 (H) | 11.43 | 1.55 | 0.083 | 17.6 |
| CHN82-20PC (3070 m) | 80–82 (G) | 22.91 | 2.91 | 0.116 | 69.0 |
| CHN82-20PC (3070 m) | 80–82 (G) | 24.96 | 3.06 | 0.134 | 60.3 |
| CHN82-20PC (3070 m) | 80–82 (G) | 9.67 | 3.25 | 0.117 | 61.1 |
| CHN82-11PG (3209 m) | 6–8 (H) | 14.51 | 1.70 | 0.084 | 13.7 |
| CHN82-11PC (3209 m) | 74–76 (G) | 19.85 | 3.62 | 0.160 | 43.6 |
| CHN82-11PC (3209 m) | 74–76 (G) | 22.95 | 4.13 | 0.157 | 39.6 |
| CHN82-11PC (3209 m) | 76–78 (G) | 16.89 | 3.50 | 0.164 | 38.0 |
| CHN82-11PC (3209 m) | 78–80 (G) | 14.03 | 3.15 | 0.135 | 32.7 |
| CHN82-11PC (3209 m) | 78–80 (G) | 23.42 | 3.08 | 0.142 | 33.0 |
| CHN82-4PG (3427 m) | 0–3 (H) | 15.20 | 1.64 | 0.097 | 23.4 |
| CHN82-4PG (3427 m) | 0–3 (H) | 17.90 | 1.65 | 0.106 | 27.7 |
| CHN82-4PC (3427 m) | 57–61 (G) | 4.20 | 3.65 | 0.179 | 73.7 |
| CHN82-4PC (3427 m) | 60–65 (G) | 12.48 | 5.03 | 0.165 | 108.9 |
| CHN82-4PC (3427 m) | 60–65 (G) | 11.05 | 4.41 | 0.159 | 125.6 |
| | | *Uvigerina spp.* | | | |
| V29-193 (1326 m) | 0–1 (H) | 11.48 | 3.56 | 0.153 | 9.2 |
| V29-204 (1849 m) | 10–12 (H) | 13.67 | 0.95 | 0.068 | 10.3 |
| V28-73 (2063 m) | 3–4 (H) | 14.55 | 2.46 | 0.133 | 15.2 |
| V28-73 (2063 m) | 10 (H) | 7.90 | 2.58 | 0.118 | 8.3 |
| CHN82-20PC (3070 m) | 80–82 (G) | 14.50 | 3.13 | 0.106 | 10.3 |
| CHN82-20PC (3070 m) | 80–82 (G) | 18.40 | 2.33 | 0.107 | 12.8 |
| CHN82-11PC (3209 m) | 74–76 (G) | 12.51 | 2.68 | 0.131 | 3.2 |
| CHN82-11PC (3209 m) | 74–76 (G) | 13.82 | 2.59 | 0.132 | 5.1 |
| CHN82-11PC (3209 m) | 76–78 (G) | 12.41 | 2.34 | 0.140 | 5.5 |
| CHN82-11PC (3209 m) | 76–78 (G) | 14.92 | 2.23 | 0.123 | 5.9 |
| CHN82-11PC (3209 m) | 78–80 (G) | 10.39 | 3.14 | 0.115 | 4.3 |
| CHN82-11PC (3209 m) | 78–80 (G) | 10.99 | 2.24 | 0.112 | 3.9 |
| CHN82-4PC (3427 m) | 57–61 (G) | 15.66 | 2.25 | 0.123 | 20.3 |
| CHN82-4PC (3427 m) | 57–61 (G) | 13.95 | 2.20 | 0.121 | 17.0 |
| CHN82-4PC (3427 m) | 60–65 (G) | 19.82 | 1.75 | 0.117 | 19.5 |
| CHN82-4PC (3427 m) | 60–65 (G) | 9.40 | 1.62 | 0.109 | 20.8 |
| | | *C. kullenbergi*[d] | | | |
| CHN82-15PC (2153 m) | 0–6 (H) | 28.58 | 7.41 | 0.084 | 7.0 |
| CHN82-11PG (3209 m) | 6–8 (H) | 16.86 | 7.93 | 0.062 | 5.8 |
| CHN82-4PG (3427 m) | 0–3 (H) | 25.04 | 9.08 | 0.073 | 6.5 |
| CHN82-4PG (3427 m) | 0–3 (H) | 17.27 | 9.91 | 0.055 | 6.0 |
| | | *C. pachyderma*[d] | | | |
| V29-193 (1326 m) | 0–1 (H) | 18.03 | 4.77 | 0.077 | 15.5 |
| | | *C. rugosus* | | | |
| CHN82-15PC (2153 m) | 0–6 (H) | 25.90 | 2.10 | 0.065 | 16.7 |
| CHN82-15PC (2153 m) | 31 (G) | 21.78 | 2.32 | 0.047 | 15.0 |

[a] Bold *C. wuellerstorfi* values are believed to be contaminated and are excluded from calculations; nm indicates that element was not measured due to insufficient sample volume.

[b] Holocene samples are indicated by H, and LGM samples are indicated by G.

[c] Sample depths are composite; actual sample IDs are 980C-2H-01, 63–64 cm and 84–86 cm.

[d] *C. kullenbergi* and *C. pachyderma* Zn/Ca values may all be contaminated, or these species may have very high Zn partition coefficients.

**Table 3.** Circulation Model Parameters for Four Deepest Cores[a]

| Modern | | | | | | | | |
|---|---|---|---|---|---|---|---|---|
| Core | Depth | Local Cd | Local Zn | Aged NADW Cd | Aged NADW Zn | NADW Cd Aging | NADW Zn Aging | Proportion SOW |
| V29-202 | 2658 | 0.208 | 1.36 | 0.202 | 1.28 | 0.042 | 0.19 | 0.013 |
| CHN82-20 | 3070 | 0.245 | 1.73 | 0.218 | 1.35 | 0.058 | 0.26 | 0.060 |
| CHN82-11 | 3209 | 0.248 | 1.78 | 0.216 | 1.34 | 0.056 | 0.25 | 0.070 |
| CHN82-4 | 3427 | 0.248 | 1.88 | 0.203 | 1.28 | 0.043 | 0.19 | 0.095 |

| Preformed | | | | | | | |
|---|---|---|---|---|---|---|---|
| Core | Depth | Cd/Ca[b] | $Cd_W$ | *Preformed NADW Cd* | *Preformed NADW Zn* | Predicted $Zn_W$ | Predicted Zn/Ca[c] |
| V29-202 | 2658 | 0.099 | 0.380 | *0.334* | *1.64* | 1.82 | 1.64 |
| CHN82-20 | 3070 | 0.122 | 0.422 | *0.348* | *1.67* | 2.15 | 1.94 |
| CHN82-11 | 3209 | 0.152 | 0.523 | *0.456* | *1.93* | 2.45 | 2.20 |
| CHN82-4 | 3427 | 0.168 | 0.578 | *0.526* | *2.03* | 2.65 | 2.39 |

| Aging | | | | | | | |
|---|---|---|---|---|---|---|---|
| Core | Depth | Cd/Ca[b] | $Cd_W$ | *NADW Cd Aging* | *NADW Zn Aging* | Predicted $Zn_W$ | Predicted Zn/Ca[c] |
| V29-202 | 2658 | 0.099 | 0.380 | *0.216* | *0.78* | 1.94 | 1.74 |
| CHN82-20 | 3070 | 0.122 | 0.422 | *0.246* | *0.85* | 2.27 | 2.05 |
| CHN82-11 | 3209 | 0.152 | 0.523 | *0.352* | *1.10* | 2.56 | 2.31 |
| CHN82-4 | 3427 | 0.168 | 0.578 | *0.409* | *1.23* | 2.82 | 2.54 |

| Mixing | | | | | | |
|---|---|---|---|---|---|---|
| Core | Depth | Cd/Ca[b] | $Cd_W$ | *Proportion SOW* | Predicted $Zn_W$ | Predicted Zn/Ca[c] |
| V29-202 | 2658 | 0.099 | 0.380 | *0.382* | 3.67 | 3.30 |
| CHN82-20 | 3070 | 0.122 | 0.422 | *0.451* | 4.15 | 3.73 |
| CHN82-11 | 3209 | 0.152 | 0.523 | *0.677* | 5.54 | 4.99 |
| CHN82-4 | 3427 | 0.168 | 0.578 | *0.804* | 6.32 | 5.69 |

| Mixing, Accounting for $\Delta CO_3^{2-}$ | | | | | | |
|---|---|---|---|---|---|---|
| Modern $[CO_3^{2-}]$ | Modern $\Delta CO_3^{2-}$ | Aged NADW $[CO_3^{2-}]$ | LGM[d] $[CO_3^{2-}]$ | LGM $\Delta CO_3^{2-}$ | Predicted $D_{Zn}$ | Predicted Zn/Ca |
| 100 | 29 | 100.3 | 92.5 | 21.5 | 8.48 | 3.11 |
| 102 | 23 | 103.4 | 92.8 | 13.8 | 7.32 | 3.04 |
| 104 | 23 | 105.8 | 88.3 | 7.3 | 6.35 | 3.52 |
| 107 | 23 | 109.9 | 85.8 | 1.8 | 5.52 | 3.49 |

[a] Modern NADW preformed Cd is 0.160 nmol $kg^{-1}$, and preformed Zn is 1.09 nmol $kg^{-1}$. Aged SOW end-member Cd is 0.669 nmol $kg^{-1}$, and Zn is 7.55 nmol $kg^{-1}$. For each model, parameters in italics are solved for by holding other parameters constant (see text). Dissolved Cd and Zn are given in nmol $kg^{-1}$; Cd/Ca and Zn/Ca are in μmol $mol^{-1}$; and $[CO_3^{2-}]$ and $\Delta CO_3^{2-}$ are in μmol $kg^{-1}$.

[b] Cd/Ca values are as measured in LGM *C. wuellerstorfi*.

[c] Zn/Ca predictions assume $D_{Zn} = 9$, except for final scenario where $\Delta CO_3^{2-}$ is accounted for.

[d] Glacial SOW end-member $[CO_3^{2-}]$ is assumed to have been 80 μmol $kg^{-1}$.

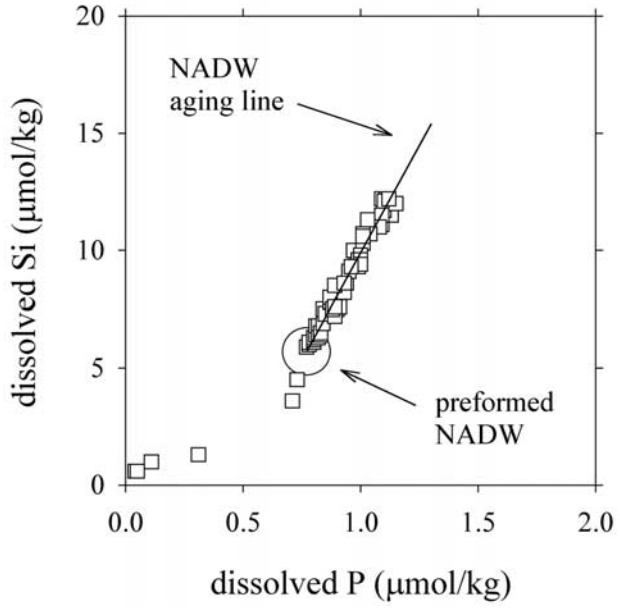


**Figure 6.** Dissolved P and Si measurements from nine North Atlantic GEOSECS stations [*Bainbridge*, 1981]. Data begin (lower left) near the region of deep convection in the Greenland Sea (station 16, 72°N, 8°W, ~1–1300 m), then follow the "core" of NADW as far south as station 1 (45°N, 42°W, ~2000 m). Line represents aging of NADW independent of mixing with waters of southern origin. The lowest point along this line (circle) is taken to represent "preformed" NADW.

NADW formation in the Greenland Sea through the core of NADW at ~2000 m (Figure 6). By a depth of about 100 m in the Greenland Sea, P and Si begin to fall along a linear aging trend that continues well into the open North Atlantic. The minimum values along this trend are chosen to represent preformed NADW (~0.77 μmol kg$^{-1}$ for P and 5.7 μmol kg$^{-1}$ for Si). The preformed P value is close to *Broecker and Peng*'s [1982] choice for preformed NCW (~0.7 μmol kg$^{-1}$). The slope of this line characterizes remineralization within "pure" NADW, with a Si:P addition ratio of about 18:1. Conversion to Cd and Zn gives preformed values of ~0.16 and 1.1 nmol kg$^{-1}$, respectively (Figure 7a). We probably overestimate the lowest Zn values (below ~1.3 nmol kg$^{-1}$) because the Zn:Si relationship of *Marchitto et al.* [2000] is based on waters deeper than 1000 m and has a positive Zn intercept (0.79 nmol kg$^{-1}$), whereas surface waters with near-zero Si generally contain negligible Zn [*Bruland et al.*, 1978]. Thus the true Zn:Cd line probably bends toward a negative y-intercept, as suggested by the Si:P plot (Figure 6), though this discrepancy has no effect on our calculations. The Zn:Cd aging trend is kinked at the same Cd concentration (0.28 nmol kg$^{-1}$) as *Boyle*'s [1988] Cd:P relationship. The slope decreases from $\Delta Zn = 4.55\Delta Cd$ before the kink to $\Delta Zn = 2.38\Delta Cd$ after the kink.

[21] Mixing at each of our four deepest cores is modeled as the simple combination of two end-members, NADW and SOW, both of which are aged beyond their preformed values prior to mixing. We do not attempt to deal with the effects of diffusion and diapycnal mixing. It is difficult to choose an appropriate aged SOW end-member because SOW aging is strongly masked by mixing with NADW in the modern ocean. We choose the maximum P and Si concentrations found in the Atlantic before dilution with NADW (~2.32 and 130 μmol kg$^{-1}$, respectively, at ~45°S, >5500 m); equivalent Cd and Zn concentrations are 0.67 and 7.6 nmol kg$^{-1}$ (Figure 7a). We recognize that these waters are too dense to be a true end-member for our cores, but their nutrient content is a best estimate for "pure" SOW. These values are slightly aged relative to *Broecker et al.*'s [1991] Southern Component Water (SCW; P ≈ 2.19 μmol kg$^{-1}$, Si ≈ 120 μmol kg$^{-1}$).

[22] The modern aged NADW end-member appropriate for CHN82-20 is determined by extrapolating the mixing line between aged SOW and the core site to the NADW aging line (Figure 7a). This gives a Cd concentration of ~0.22 nmol kg$^{-1}$ and a Zn concentration of ~1.4 nmol kg$^{-1}$, equivalent to the P and Si values of *Broecker et al.*'s [1991] NCW. By this scheme, modern waters at CHN82-20 are about 6% SOW. This is similar to *Broecker et al.*'s [1991] estimate based on the conservative tracer $PO_4^*$, which puts the region of CHN82-20 about midway between the 0% and 10% SCW contours.

### 4.4. Three Glacial Circulation Models

[23] For each of our LGM scenarios (preformed nutrients, NADW aging, and mixing with SOW) we alter one process and hold the other two processes at modern levels. Note that we do not use GNAIW as an end-member for the deep cores, but rather some form of NADW with nutrient contents that we will model. In each case, we solve simple equations of the general form:

$$N(\mathrm{p}+\mathrm{a}) + S(\mathrm{s}) = \mathrm{c} \qquad (1)$$

where $N$ and $S$ are the proportions of NADW and SOW, p is the NADW preformed nutrient (Cd or Zn) concentration, a is the aging component, s is the aged SOW nutrient concentration, and c is the nutrient concentration at the core site.

[24] For the sake of simplicity, we hold the aged SOW end-member at its modern nutrient coordinates (s) for all three scenarios. Additional aging beyond these values would presumably occur during the northward progression of SOW in the absence of NADW. However, because the northern and southern end-members have such disparate nutrient contents relative to the likely magnitude of unaccounted-for aging, the resulting error should be small. Another potential error surrounds the initial composition of glacial SOW before it leaves the Southern Ocean. LGM deep Southern Ocean $\delta^{13}C$ values, even after discarding cores suspected of being biased by productivity artifacts, were at least 0.5–0.8‰ lower than today [*Mackensen et al.*, 1993; *Matsumoto and Lynch-Stieglitz*, 1999]. If mean ocean $\delta^{13}C$ was ~0.3‰ lower than modern [*Duplessy et al.*, 1988], this implies either an increase in nutrients or a decrease in the air-sea exchange component of $\delta^{13}C$ ($\delta^{13}C_{as}$) [*Lynch-Stieglitz and Fairbanks*, 1994]. If nutrient-related, some of the change may simply be due to a decreased influence of low-nutrient NADW on CPDW

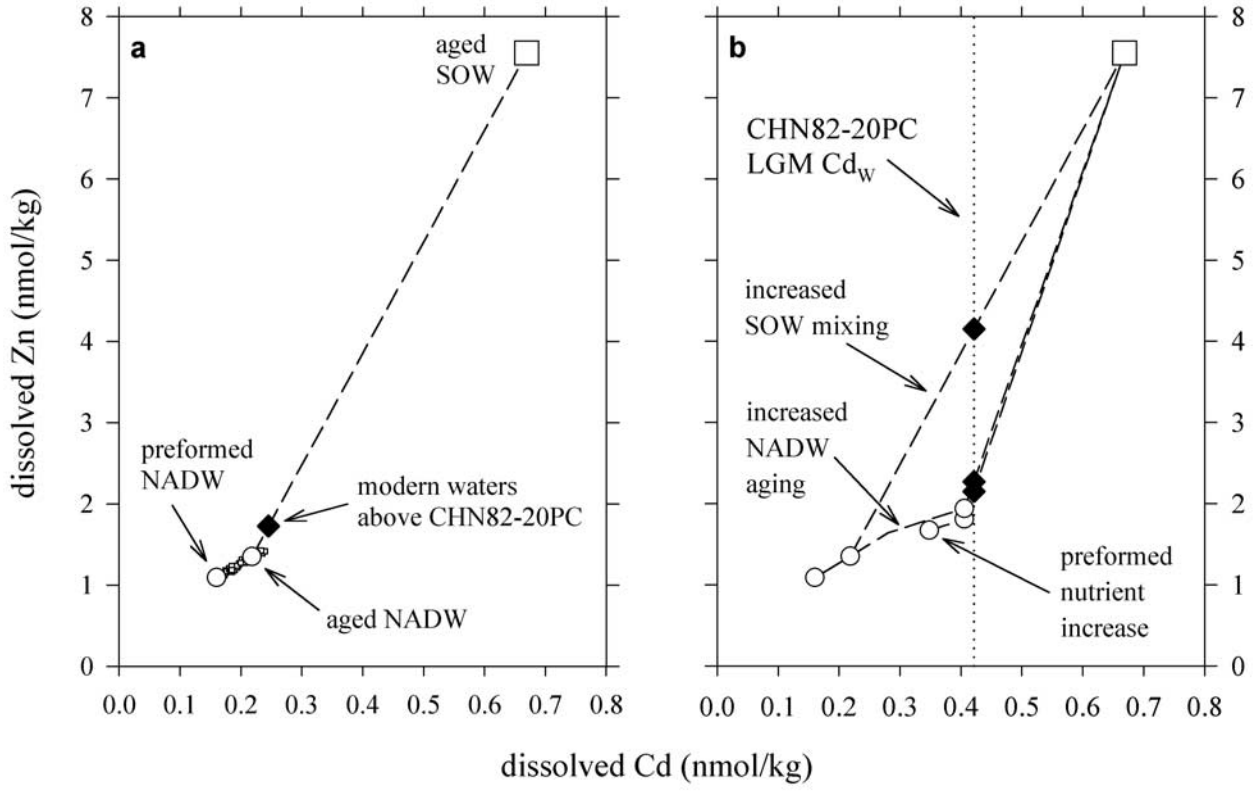


**Figure 7.** (a) Modern mixing diagram for the site of core CHN82-20PC. Dissolved P and Si data from Figure 8 have been converted to Cd and Zn, respectively (small squares). The CHN82-20PC coordinates (diamond) are taken from P and Si at GEOSECS station 27 (42°N, 42°W) [*Bainbridge*, 1981]. The "aged SOW" end-member (large square) is taken from GEOSECS station 67 (45°S, 51°W, >5500 m). The "aged NADW" end-member that is appropriate for CHN82-20PC is calculated by extending the mixing line between SOW and the core site (dashed line) to the NADW aging line. (b) LGM mixing diagram for core CHN82-20PC. The LGM $Cd_W$ value in this core is shown by the vertical dotted line. The two circles in the lower left corner are the modern preformed and aged NADW end-members, as in Figure 7a. The remaining dashed lines show the three glacial circulation scenarios discussed in the text. The intersection of these lines with the $Cd_W$ line gives predicted seawater Zn concentrations (diamonds).

properties [*Oppo and Fairbanks*, 1987]. Although Southern Ocean Cd/Ca data suggest no significant difference from today [*Boyle*, 1992; *Boyle and Rosenthal*, 1996] (implying a $\delta^{13}C_{as}$ change), it is conceivable that some of these values are reduced by a $\Delta CO_3^{2-}$ artifact [*McCorkle et al.*, 1995]. If the glacial $\delta^{13}C$ drop indeed reflects an increase in SOW nutrients, then the SOW Zn:Cd coordinates in Figure 7b would migrate to the upper right; this would have the same effect as unaccounted-for SOW aging, with little impact on our results (see section 4.5). Another possibility is that $\Sigma CO_2$ accumulated in the deep Southern Ocean independent of nutrients [*Toggweiler*, 1999], leading to lower $\delta^{13}C$ without higher Cd or Zn.

[25] We assume that the glacial NADW aging process followed the same kinked Zn:Cd trend as today. One might argue that since little aging is observed within modern NADW, the modern deep Pacific would offer a better analog for hypothesized glacial NADW aging. We contend that the steeper Zn:Cd aging slope of the modern Pacific depends to a large degree on a greater supply of Zn to the surface ocean (and its subsequent removal by biogenic particles). Therefore if glacial North Atlantic preformed nutrients were as low as today (as assumed in the increased aging and mixing scenarios below), or if the preformed Zn:Cd ratio remained low (as argued in the preformed nutrients scenario below), then modern NADW is a better analog for aging than the deep Pacific.

[26] A final source of uncertainty concerns the glacial whole-ocean inventories of Cd and Zn. If one or both were very different from today, then our various assumptions for the LGM scenarios would be violated. *Boyle* [1992] estimated that the LGM Cd inventory was perhaps 10% lower, but noted that the uncertainty is of the same order as the estimate. Aside from the North Atlantic data presented here, the only Zn/Ca measurements for the glacial ocean are from two cores in the deep eastern equatorial Pacific [*Marchitto et al.*, 2001]. Comparison to paired Cd/Ca measurements suggests that LGM Zn concentrations were probably within ±25% of modern levels. To the extent that deep equatorial Pacific waters reflect the global ocean, our best guess is that

the global Zn inventory was not drastically different from today. Clearly this assumption will require additional verification in the future.

#### 4.4.1. Increased preformed nutrients

[27] To model the first LGM scenario, increased preformed nutrients, NADW aging and SOW mixing are held at modern levels. At CHN82-20 this means a Cd aging of 0.06 nmol $kg^{-1}$ over the unspecified preformed value and a 6% admixture of SOW. These constraints require a preformed Cd concentration of 0.35 nmol $kg^{-1}$, more than double the modern value, to yield a glacial Cd concentration of 0.42 nmol $kg^{-1}$ (based on the measured Cd/Ca value). Algebraically,

$$0.94(p + 0.06) + 0.06(0.67) = 0.42 \quad (2)$$

where 0.94 and 0.06 are the proportions of NADW and SOW, p is the NADW preformed Cd concentration, 0.06 is the aging component, and 0.67 is the SOW Cd concentration. The only logical source for such elevated preformed NADW nutrients (aside from upwelled deep SOW) is midlatitude intermediate waters, where Cd concentrations of ~0.35 nmol $kg^{-1}$ (P = 1.5 μmol $kg^{-1}$) are found as far north as 27°N today [*Bainbridge*, 1981] (see Figure 1). This general region supplies the "feed water" for modern NADW [*Broecker and Peng*, 1982]. However, the available LGM (non-Heinrich) Cd/Ca data from the mid to low-latitude North Atlantic suggest that intermediate and shallow waters were depleted in Cd relative to today [*Boyle*, 1992; *Marchitto et al.*, 1998; *Williamowski and Zahn*, 2000; *Zahn and Stüber*, 2002]. It is therefore difficult to imagine how high Cd concentrations could have extended to the shallow, higher latitude North Atlantic without impacting lower latitudes.

[28] Regardless of the hypothetical route, concomitant preformed NADW Zn increases can be estimated by looking to Zn:Cd ratios in the presumed source (midlatitude intermediate waters). In the modern ocean, a Cd concentration of 0.35 nmol $kg^{-1}$ is expected to be accompanied by a Zn concentration of only ~1.7 nmol $kg^{-1}$ (see Figure 1). This low Zn:Cd ratio is predominately set by the differential regeneration depths of the two elements (i.e., these waters collect much more regenerated Cd than Zn). The relatively high Zn:Cd ratio in Antarctic Intermediate Water (AAIW) has little influence because of AAIW's minor contribution to Northern Hemisphere waters (<10% above 20°N [*Wüst*, 1935; *Broecker and Takahashi*, 1981]), and it appears to have had no greater influence at the LGM [*Boyle*, 1992; *Marchitto et al.*, 1998; *Williamowski and Zahn*, 2000; *Zahn and Stüber*, 2002]. We therefore take the modern value of 1.7 nmol $kg^{-1}$ as a reasonable estimate for the LGM preformed Zn concentration. Note that the influence of AAIW may have increased during Heinrich events [*Williamowski and Zahn*, 2000; *Zahn and Stüber*, 2002], though we suspect that the differential biogeochemistry of Zn and Cd still kept the Zn:Cd ratio of North Atlantic intermediate waters relatively low.

[29] Since our inferred LGM preformed concentrations are beyond the presumed kink in the Zn:Cd aging relationship, we convert the constant NADW Cd aging (0.06 nmol $kg^{-1}$ beyond the preformed value) to equivalent Zn aging (0.1 nmol $kg^{-1}$) using the post-kink slope ($\Delta Zn = 2.38\Delta Cd$) (Figure 7b). By again assuming constant mixing (6% SOW), the resulting LGM Zn concentration at CHN82-20 can be predicted:

$$0.94(1.7 + 0.1) + 0.06(7.6) = c \quad (3)$$

where c is the CHN82-20 Zn concentration, equal to 2.2 nmol $kg^{-1}$ (Figure 7b). Thus the maximum ($D_{Zn}$ = 9) LGM Zn/Ca value predicted by this circulation scenario is 1.9 μmol $mol^{-1}$. This is about 40% lower than the measured value of 3.07 ± 0.17 μmol $mol^{-1}$.

#### 4.4.2. Increased NADW aging

[30] For the second LGM scenario, increased NADW aging, preformed nutrients are held constant (Cd = 0.16 nmol $kg^{-1}$) and mixing with SOW is again held constant (6% SOW). The amount of Cd addition from remineralization within the North Atlantic (aging) required to reach the LGM concentration at CHN82-20 is therefore 0.25 nmol $kg^{-1}$, more than four times the modern estimate:

$$0.94(0.16 + a) + 0.06(0.67) = 0.42 \quad (4)$$

Assuming that Zn was added along with Cd following the kinked aging trend ($\Delta Zn = 4.55\Delta Cd$ below Cd = 0.28 nmol $kg^{-1}$ and $\Delta Zn = 2.38\Delta Cd$ above), this suggests that Zn increased by ~0.8 nmol $kg^{-1}$ over the constant preformed value of 1.1 nmol $kg^{-1}$. The result is a CHN82-20 concentration of 2.3 nmol $kg^{-1}$ (Figure 7b):

$$0.94(1.1 + 0.8) + 0.06(7.6) = c \quad (5)$$

This circulation scheme therefore predicts that LGM Zn/Ca at CHN82-20 should be no higher than 2.0 μmol $mol^{-1}$ (for $D_{Zn}$ = 9), similar to the estimate from the first model.

#### 4.4.3. Increased mixing with SOW

[31] The final circulation scenario, increased mixing with SOW, has the potential to result in significantly higher Zn concentrations at CHN82-20. This is because deep SOW contains much more Zn than North Atlantic intermediate and surface waters, which were the sources of increased nutrients in the first two schemes. For the increased mixing model, preformed nutrients and NADW aging are both held constant. These constraints require a 45% contribution from SOW to give the LGM Cd concentration at CHN82-20:

$$(1 - S)(0.16 + 0.06) + S(0.67) = 0.42 \quad (6)$$

This dramatic SOW increase predicts a CHN82-20 Zn concentration of 4.1 nmol $kg^{-1}$ (Figure 7b):

$$0.55(1.1 + 0.3) + 0.45(7.6) = c \quad (7)$$

where the Zn aging component (0.3 nmol $kg^{-1}$) is based on the prekink Zn:Cd slope ($\Delta Zn = 4.55\Delta Cd$).

[32] The resulting maximum ($D_{Zn}$ = 9) Zn/Ca value is therefore 3.7 μmol $mol^{-1}$, almost double the previous two predictions. However, because $D_{Zn}$ is a function of $\Delta CO_3^{2-}$ [*Marchitto et al.*, 2000], the increased influence of low-$CO_3^{2-}$ SOW would be expected to reduce this number somewhat. The modern $CO_3^{2-}$ concentration at CHN82-20 is ~102 μmol $kg^{-1}$ (calculated from nearest GEOSECS data). An increase in the admixture of SOW ($CO_3^{2-} \approx 80$ μmol $kg^{-1}$,

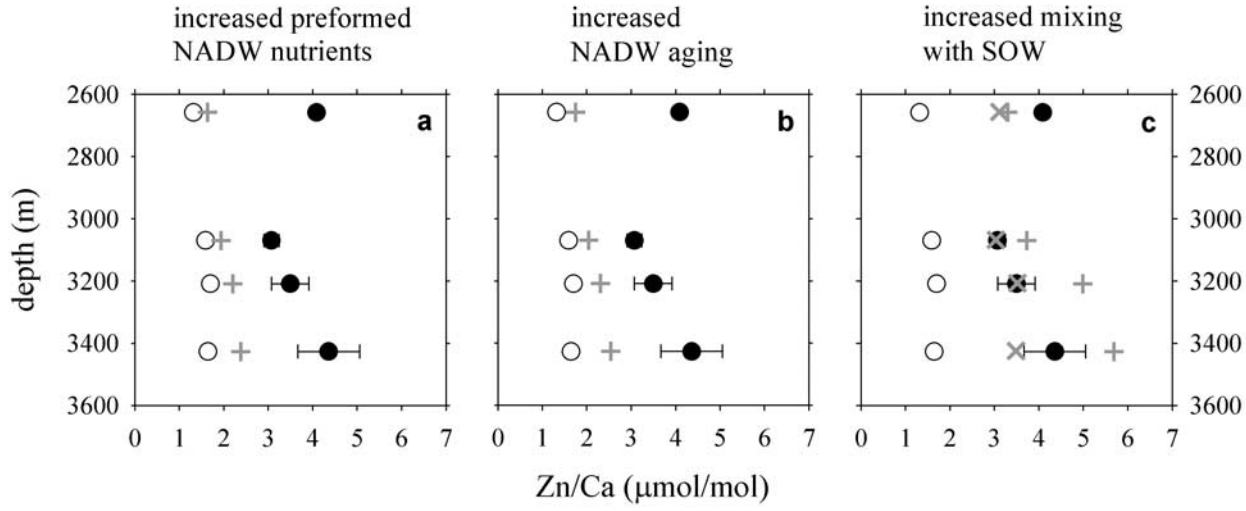


**Figure 8.** Three models used to simulate LGM *C. wuellerstorfi* Zn/Ca values in the four deepest cores. Open circles are observed Holocene values, and solid circles are observed LGM values. Pluses show the LGM predictions of each model. The results of (a) increased preformed nutrients and (b) increased aging are much lower than the observations. The results of increased mixing with SOW are mostly higher than the LGM observations if the saturation state of the bottom water is unaccounted for (pluses in Figure 8c). But since the encroachment of low-$CO_3^{2-}$ SOW would also lower the partition coefficients for Zn into foraminiferal calcite, the true predictions (crosses in Figure 8c) are somewhat lower and therefore in best agreement with the observed values.

assumed to be roughly the same as today) from the modern 6% to the glacial 45% would lower CHN82-20 to ~93 μmol $kg^{-1}$. Thus $\Delta CO_3^{2-}$ would have dropped from 23 μmol $kg^{-1}$ to ~14 μmol $kg^{-1}$ (assuming negligible change in $[CO_3^{2-}]_{saturation}$); this corresponds to a $D_{Zn}$ of 7.3 and a predicted Zn/Ca of 3.0 μmol $mol^{-1}$, indistinguishable from the measured value (3.07 ± 0.17 μmol $mol^{-1}$).

### 4.5. Zn/Ca Data and Model Comparison

[33] In Figure 8, measured Zn/Ca values from all four deep cores are compared to values predicted by each of the three glacial circulation models. The first two models (increased preformed nutrients and increased aging) clearly underestimate Zn/Ca at all depths. Maximum predictions of the mixing model ($D_{Zn}$ = 9) significantly overestimate Zn/Ca in the three deepest cores and underestimate it in the 2658 m core. However, predictions are in good agreement with the three deepest cores when the effect of reduced $CO_3^{2-}$ concentration is incorporated into the mixing model. It is possible that the single glacial analysis at 2658 m is affected by Zn contamination.

[34] Overall, the combined Cd/Ca and Zn/Ca data strongly argue for the increased influence of SOW during the LGM. Estimates range from 38% SOW at 2658 m to 80% SOW at 3427. Because the mixing model does not adequately account for SOW aging within the glacial Atlantic (nor a possible increase in preformed SOW), these numbers are more relative than absolute. In other words, by the time it got to ~42°N, the true nutrient content of aged glacial SOW was probably somewhat higher than the chosen end-member composition, meaning that 80% is likely an overestimate of the actual mixing. This uncertainty should have a small effect on the seawater Zn concentrations predicted from Cd/Ca (equation 7) because a lower SOW percentage would be compensated by a higher SOW Zn value.

[35] The most likely explanation for the increased admixture of SOW in the deep North Atlantic is a reduction in NADW formation, though clearly not a cessation. This reduction appears to have been at least partially balanced by the formation of GNAIW. Sedimentary $^{231}Pa/^{230}Th$ ratios suggest that the rate of GNAIW export to CPDW was similar to or even slightly greater than that of modern NADW [*Yu et al.*, 1996]. In contrast, *Lynch-Stieglitz et al.* [1999] argue that a large glacial reduction in Gulf Stream transport through the Florida Straits (calculated from benthic $\delta^{18}O$ using the geostrophic method) was probably caused by a near cessation of southward deep/intermediate water flow, implying very weak GNAIW transport. In either case, glacial cooling in the North Atlantic would have been compounded because GNAIW was a less efficient "heat pump" than NADW is [*Rahmstorf*, 1994]. The forcing for this rearrangement is believed to have been lowered North Atlantic sea surface salinities, resulting in lower densities for sinking waters [*Broecker et al.*, 1985]. However, the deep ocean paleonutrient data only address the *relative* influences of northern and southern components [*Boyle and Keigwin*, 1982]. It is therefore possible that the main forcing actually occurred in the Southern Ocean, with increased AABW production displacing NADW to a shallower level, though it is unclear what effect this might have had on North Atlantic climate. We favor the conventional view of North Atlantic salinity forcing because it is strongly supported by ocean circulation models [e.g., *Stocker and Wright*, 1991; *Mikolajewicz and Maier-Reimer*, 1994;

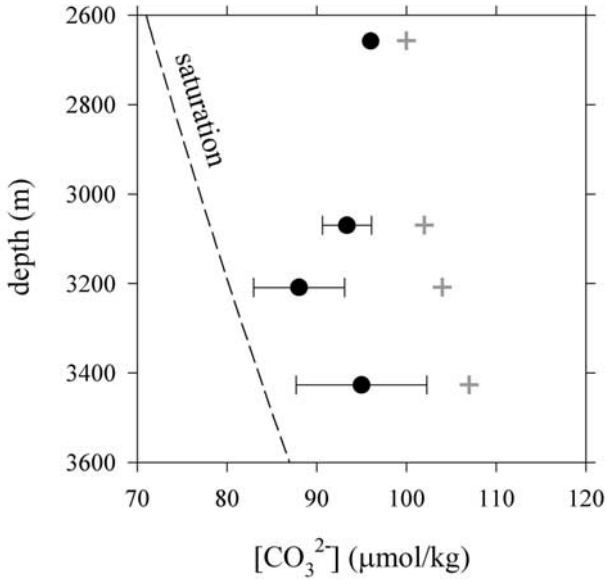


**Figure 9.** Carbonate ion concentrations calculated from GEOSECS data (pluses) and estimated from LGM Zn/Ca data combined with seawater [Zn] predictions based on Cd/Ca (circles). Error bars account for Zn/Ca scatter only. Shallowest LGM point is a minimum value, corresponding to an inferred $D_{Zn}$ close to 9. Dashed line shows the modern $[CO_3^{2-}]$ for saturation with respect to calcite.

*Rahmstorf*, 1995; *Tziperman*, 1997]. In particular, the inherent instability of a North Atlantic thermohaline circulation weakened by freshwater is consistent with the climatic variability of glacial periods [e.g., *Tziperman*, 1997]. Of course, even this North Atlantic forcing would not rule out a concurrent increase in AABW production.

[36] Regardless of forcing mechanisms, the dissolved Zn estimates derived from Cd/Ca can be combined with Zn/Ca data to infer glacial $\Delta CO_3^{2-}$ values (via inferred $D_{Zn}$):

$$\Delta CO_3^{2-} = (D_{Zn} - 5.25)/0.15 \quad (8)$$

This equation is valid up to $D_{Zn}$ = 9 and $\Delta CO_3^{2-}$ = 25 μmol kg$^{-1}$ [*Marchitto et al.*, 2000]. LGM $\Delta CO_3^{2-}$ results range from ≥25 μmol kg$^{-1}$ at 2658 m to ~7 μmol kg$^{-1}$ at 3209 m. Assuming negligible changes in $[CO_3^{2-}]_{saturation}$, these values suggest that $[CO_3^{2-}]_{in\ situ}$ dropped by a range of ≤4 μmol kg$^{-1}$ at 2658 m to ~16 μmol kg$^{-1}$ at 3209 m (Figure 9). The mean decrease below 3000 m is 12 μmol kg$^{-1}$, of the same order as previous deep Atlantic estimates based on $CaCO_3$ preservation [*Broecker*, 1995]. However, we do not see evidence of the steep vertical $CO_3^{2-}$ gradient recently reconstructed by *Broecker and Clark* [2001] using planktonic foraminiferal weights. As discussed above, our inferred decrease is consistent with the admixture of relatively corrosive (low-$CO_3^{2-}$) SOW. Given all of the uncertainties involved, however, the present numbers should be taken as crude estimates only.

### 4.6. Alternate Treatment of the Data

[37] One could argue for at least two alternate ways to carry out the above modeling of the four deepest cores. First, as mentioned above, the kinked Cd:P relationship of *Boyle* [1988] could be replaced with the Atlantic curve of *Elderfield and Rickaby* [2000]. For all three LGM scenarios, the Zn/Ca predictions based on Cd/Ca would be slightly higher with the curved model (SOW end-member Cd is not recalculated because modern Southern Ocean waters are better described by the kinked model). Zn/Ca differences from the kinked model would be +7–8% for the preformed scenario and +7–11% for the aging scenario. In each case, model predictions would still be significantly lower than observed Zn/Ca values (see Figure 8). The increased mixing with SOW scenario would rise by just 2–6% (assuming a $D_{Zn}$ of 9), or +1–5% after accounting for reduced $\Delta CO_3^{2-}$.

[38] Second, rather than using the $Cd_W$ values calculated directly from LGM Cd/Ca, one could calculate the $Cd_W$ difference between LGM and Holocene samples and then add that to the modern Cd predicted from P. This strategy might be valid if the Holocene data, which are slightly higher than predicted, are indicative of some foraminiferal offset that also applies to the glacial data (we consider it more likely that the Holocene samples that we have measured are not quite characteristic of modern conditions, due to slow sedimentation rates and missing core tops). Zn/Ca predictions of all three scenarios would be lower using this LGM-Holocene difference method. For the preformed (6–13% decrease) and aging (4–12% decrease) scenarios, predictions would be even farther away from measured values. For increased mixing with SOW, Zn/Ca predictions using a partition coefficient of 9 would be 10–36% lower than before and inferred SOW percentages would drop to 17–58%. Measured Zn/Ca values in the three deepest cores are only slightly lower than these predictions and therefore would require little lowering of $\Delta CO_3^{2-}$. Thus the data would still argue strongly for the presence of SOW, but evidence for the expected drop in $[CO_3^{2-}]$ would be lacking.

## 5. Conclusions

[39] *C. wuellerstorfi* Cd/Ca data from the North Atlantic suggest large increases in deep water nutrient contents during the LGM. In theory, such changes could have resulted from: (1) increased preformed nutrients in the high-latitude North Atlantic; (2) increased aging of lower NADW; or (3) decreased relative production of NADW and greater mixing with SOW. Zn/Ca data from the same samples are too high to be explained by the first two mechanisms. They require that SOW was a major contributor to the glacial North Atlantic deeper than about 2500 m, consistent with a partial replacement of NADW by GNAIW. However, since the paleonutrient data only address relative influences of NADW and SOW, an increase in AABW formation could have also contributed. With this increased SOW influence came a significant lowering of deep North Atlantic $CO_3^{2-}$ concentrations, on the order of 10 to 15 μmol kg$^{-1}$.

[40] Although previous interpretations of $\delta^{13}C$, Cd/Ca, and Ba/Ca data appear to be generally valid in terms of reduced NADW formation during the LGM, much com-

plexity remains. A better understanding of the effects of $\Delta CO_3^{2-}$ on benthic foraminiferal chemistry [*McCorkle et al.*, 1995; *Marchitto et al.*, 2000] is essential for reconstructing the details of glacial deep circulation. Further research into the controls on planktonic foraminiferal Cd/Ca and $\delta^{13}C$ would also be useful for constraining glacial $\delta^{13}C_{as}$, which is crucial for interpreting benthic $\delta^{13}C$ data. Finally, the LGM Zn/Ca data presented here are the first published measurements for the pre-Holocene deep ocean (excepting a single glacial *Pyrgo* measurement by *Boyle* [1981]). Future estimates of the glacial oceanic inventory of dissolved Zn, perhaps bolstered by Zn/Si measurements in biogenic opal [*Ellwood and Hunter*, 2000], are therefore required to confirm and refine our results.

[41] **Acknowledgments.** We thank M. Jeglinski, D. Ostermann, and L. Zhou for assistance with core sampling and stable isotope analyses. E. Boyle, L. Keigwin, J. Lynch-Stieglitz, D. McCorkle, R. Zahn, and two anonymous reviewers contributed valuable comments and discussions that improved this manuscript. R/V *Chain* cores are curated at WHOI with support from the National Science Foundation, the Office of Naval Research, and the United States Geological Survey. R/V *Vema* cores are curated at LDEO with support from the National Science Foundation and the Office of Naval Research. This work was supported by a JOI/USSAC Ocean Drilling Fellowship (JSG-CY 12-4), the R. H. Cole Ocean Ventures Fund, and the National Science Foundation (grant OCE-9503135 to W. Curry and grant OCE-9633499 to D. Oppo). This is LDEO contribution number 6310 and WHOI contribution number 10667.

## References


Bainbridge, A. E., *GEOSECS Atlantic Expedition*, vol. 1, *Hydrographic Data*, U.S. Gov. Print. Off., Washington, D. C., 1981.

Bertram, C. J., H. Elderfield, N. J. Shackleton, and J. A. MacDonald, Cadmium/calcium and carbon isotope reconstructions of the glacial northeast Atlantic Ocean, *Paleoceanography*, *10*, 563–578, 1995.

Beveridge, N. A. S., H. Elderfield, and N. J. Shackleton, Deep thermohaline circulation in the low-latitude Atlantic during the last glacial, *Paleoceanography*, *10*, 643–660, 1995.

Boyle, E. A., Cadmium, zinc, copper, and barium in foraminifera tests, *Earth Planet. Sci. Lett.*, *53*, 11–35, 1981.

Boyle, E. A., Cadmium: Chemical tracer of deepwater paleoceanography, *Paleoceanography*, *3*, 471–489, 1988.

Boyle, E. A., Cadmium and $\delta^{13}C$ paleochemical ocean distributions during the stage 2 glacial maximum, *Annu. Rev. Earth Planet. Sci.*, *20*, 245–287, 1992.

Boyle, E. A., Limits on benthic foraminiferal chemical analyses as precise measures of environmental properties, *J. Foraminiferal Res.*, *25*, 4–13, 1995.

Boyle, E. A., and L. D. Keigwin, Deep circulation of the North Atlantic over the last 200,000 years: Geochemical evidence, *Science*, *218*, 784–787, 1982.

Boyle, E. A., and L. D. Keigwin, Comparison of Atlantic and Pacific paleochemical records for the last 215,000 years: Changes in deep ocean circulation and chemical inventories, *Earth Planet. Sci. Lett.*, *76*, 135–150, 1985/1986.

Boyle, E. A., and L. D. Keigwin, North Atlantic thermohaline circulation during the last 20,000 years linked to high latitude surface temperature, *Nature*, *330*, 35–40, 1987.

Boyle, E. A., and Y. Rosenthal, Chemical hydrography of the South Atlantic during the Last Glacial Maximum: Cd vs. $\delta^{13}C$, in *The South Atlantic: Present and Past Circulation*, edited by G. Wefer et al., pp. 423–443, Springer-Verlag, New York, 1996.

Boyle, E. A., F. R. Sclater, and J. M. Edmond, On the marine geochemistry of cadmium, *Nature*, *263*, 42–44, 1976.

Broecker, W. S., *The Glacial World According to Wally*, Lamont-Doherty Earth Obs., Palisades, N. Y., 1995.

Broecker, W. S., and E. Clark, Glacial-to-Holocene redistribution of carbonate ion in the deep sea, *Science*, *294*, 2152–2155, 2001.

Broecker, W. S., and T.-H. Peng, *Tracers in the Sea*, Lamont-Doherty Earth Obs., Palisades, N. Y., 1982.

Broecker, W. S., and T. Takahashi, Hydrography of the central Atlantic, IV, Intermediate waters of Antarctic origin, *Deep Sea Res.*, *28*, 177–193, 1981.

Broecker, W. S., D. M. Peteet, and D. Rind, Does the ocean-atmosphere system have more than one stable mode of operation?, *Nature*, *315*, 21–25, 1985.

Broecker, W. S., S. Blanton, W. M. Smethie, and G. Ostlund, Radiocarbon decay and oxygen utilization in the deep Atlantic Ocean, *Global Biogeochem. Cycles*, *5*, 87–117, 1991.

Bruland, K. W., Oceanographic distributions of cadmium, zinc, nickel, and copper in the North Pacific, *Earth Plan. Sci. Lett.*, *47*, 176–198, 1980.

Bruland, K. W., G. A. Knauer, and J. H. Martin, Zinc in north-east Pacific water, *Nature*, *271*, 741–743, 1978.

Chan, L. H., D. Drummond, J. M. Edmond, and B. Grant, On the barium data from the Atlantic GEOSECS expedition, *Deep Sea Res.*, *24*, 613–649, 1977.

Craig, H., Isotopic standards for carbon and oxygen and correction factors for mass-spectrometric analysis of carbon dioxide, *Geochim. Cosmochim. Acta*, *12*, 133–149, 1957.

Curry, W. B., and G. P. Lohmann, Carbon isotopic changes in benthic foraminifera from the western South Atlantic: Reconstruction of glacial abyssal circulation patterns, *Quat. Res.*, *18*, 218–235, 1982.

Curry, W. B., T. M. Marchitto, J. F. McManus, D. W. Oppo, and K. L. Laarkamp, Millennial-scale changes in ventilation of the thermocline, intermediate, and deep waters of the glacial North Atlantic, in *Mechanisms of Global Climate Change at Millennial Time Scales, Geophys. Monogr. Ser.*, vol. 112, edited by P. U. Clark, R. S. Webb, and L. D. Keigwin, pp. 59–76, AGU, Washington, D. C., 1999.

Duplessy, J.-C., L. Cherrouard, and F. Vila, Weyl's theory of glaciation supported by isotopic study of Norwegian core K11, *Science*, *188*, 1208–1209, 1975.

Duplessy, J.-C., N. J. Shackleton, R. G. Fairbanks, L. Labeyrie, D. Oppo, and N. Kallel, Deepwater source variations during the last climatic cycle and their impact on the global deepwater circulation, *Paleoceanography*, *3*, 343–360, 1988.

Elderfield, H., and R. E. M. Rickaby, Oceanic Cd/P ratio and nutrient utilization in the glacial Southern Ocean, *Nature*, *405*, 305–310, 2000.

Elderfield, H., C. J. Bertram, and J. Erez, A biomineralization model for the incorporation of trace elements into foraminiferal calcium carbonate, *Earth Planet. Sci. Lett.*, *142*, 409–423, 1996.

Ellwood, M. J., and K. A. Hunter, Variations in the Zn/Si record over the last interglacial glacial transition, *Paleoceanography*, *15*, 506–514, 2000.

Haskell, B. J., T. C. Johnson, and W. J. Showers, Fluctuations in deep western North Atlantic circulation on the Blake Outer Ridge during the last deglaciation, *Paleoceanography*, *6*, 21–31, 1991.

Keigwin, L. D., and E. A. Boyle, Late Quaternary paleochemistry of high-latitude surface waters, *Palaeogeogr. Palaeoclimatol. Palaeoecol.*, *73*, 85–106, 1989.

Keigwin, L. D., and S. J. Lehman, Deep circulation change linked to Heinrich event 1 and Younger Dryas in a middepth North Atlantic core, *Paleoceanography*, *9*, 185–194, 1994.

Kohfeld, K. E., R. F. Anderson, and J. Lynch-Stieglitz, Carbon isotopic disequilibrium in polar planktonic foraminifera and its impact on modern and Last Glacial Maximum reconstructions, *Paleoceanography*, *15*, 53–64, 2000.

Kroopnick, P. M., The distribution of $^{13}C$ of $\Sigma CO_2$ in the world oceans, *Deep Sea Res.*, *32*, 57–84, 1985.

Lea, D. W., and E. A. Boyle, Foraminiferal reconstruction of barium distributions in water masses of the glacial oceans, *Paleoceanography*, *5*, 719–742, 1990.

Ledbetter, M. T., and W. L. Balsam, Paleoceanography of the Deep Western Boundary Undercurrent on the North American continental margin for the past 25,000 yr, *Geology*, *13*, 181–184, 1985.

LeGrand, P., and C. Wunsch, Constraints from paleotracer data on the North Atlantic circulation during the Last Glacial Maximum, *Paleoceanography*, *10*, 1011–1046, 1995.

Lutze, G. F., and H. Thiel, Epibenthic foraminifera from elevated microhabitats: *Cibicidoides wuellerstorfi* and *Planulina ariminensis*, *J. Foram. Res.*, *19*, 153–158, 1989.

Lynch-Stieglitz, J., and R. G. Fairbanks, A conservative tracer for glacial ocean circulation from carbon isotope and palaeo-nutrient measurements in benthic foraminifera, *Nature*, *369*, 308–310, 1994.

Lynch-Stieglitz, J., W. B. Curry, and N. Slowey, Weaker Gulf Stream in the Florida Straits during the Last Glacial Maximum, *Nature*, *402*, 644–648, 1999.

Mackensen, A., H.-W. Hubberten, T. Bickert, G. Fischer, and D. K. Fütterer, The $\delta^{13}C$ in

benthic foraminiferal tests of *Fontbotia wuellerstorfi* (Schwager) relative to the $\delta^{13}C$ of dissolved inorganic carbon in Southern Ocean deep water: Implications for glacial ocean circulation models, *Paleoceanography*, *8*, 587–610, 1993.

Marchitto, T. M., W. B. Curry, and D. W. Oppo, Millennial-scale changes in North Atlantic circulation since the last glaciation, *Nature*, *393*, 557–561, 1998.

Marchitto, T. M., W. B. Curry, and D. W. Oppo, Zinc concentrations in benthic foraminifera reflect seawater chemistry, *Paleoceanography*, *15*, 299–306, 2000.

Marchitto, T. M., J. Lynch-Stieglitz, W. B. Curry, and D. W. Oppo, Quantitative reconstruction of glacial/interglacial carbonate ion concentrations in the deep Pacific using Zn and Cd in benthic foraminifera, *Eos Trans. AGU*, *82*(47), Fall Meet. Suppl., abstract OS31E-03, 2001.

Martin, P. A., and D. W. Lea, Comparison of water mass changes in the deep tropical Atlantic derived from Cd/Ca and carbon isotope records: Implications for changing Ba composition of deep Atlantic water masses, *Paleoceanography*, *13*, 572–585, 1998.

Martin, W. R., and F. L. Sayles, $CaCO_3$ dissolution in sediments of the Ceara Rise, western equatorial Atlantic, *Geochim. Cosmochim. Acta*, *60*, 243–263, 1996.

Matsumoto, K., and J. Lynch-Stieglitz, Similar glacial and Holocene deep water circulation inferred from southeast Pacific benthic foraminiferal carbon isotope composition, *Paleoceanography*, *14*, 149–163, 1999.

McCave, I. N., B. Manighetti, and N. A. S. Beveridge, Circulation in the glacial North Atlantic inferred from grain-size measurements, *Nature*, *374*, 149–152, 1995.

McCorkle, D. C., P. A. Martin, D. W. Lea, and G. P. Klinkhammer, Evidence of a dissolution effect on benthic foraminiferal shell chemistry: $\delta^{13}C$, Cd/Ca, Ba/Ca, and Sr/Ca results from the Ontong Java Plateau, *Paleoceanography*, *10*, 699–714, 1995.

McCorkle, D. M., B. H. Corliss, and C. A. Farnham, Vertical distributions and stable isotopic compositions of live (stained) benthic foraminifera from the North Carolina and California continental margins, *Deep Sea Res., Part I*, *44*, 983–1024, 1997.

McManus, J. F., D. W. Oppo, and J. L. Cullen, A 0.5-million-year record of millennial-scale climate variability in the North Atlantic, *Science*, *283*, 971–975, 1999.

Mikolajewicz, U., and E. Maier-Reimer, Mixed boundary conditions in ocean general circulation models and their influence on the stability of the model's conveyor belt, *J. Geophys. Res.*, *99*, 22,633–22,644, 1994.

Mix, A. C., and R. G. Fairbanks, North Atlantic surface-ocean control of Pleistocene deep-ocean circulation, *Earth Planet. Sci. Lett.*, *73*, 231–243, 1985.

Newell, R. E., Changes in the poleward energy flux by the atmosphere and ocean as a possible cause for ice ages, *Quat. Res.*, *4*, 117–127, 1974.

Oppo, D. W., and R. G. Fairbanks, Variability in the deep and intermediate water circulation of the Atlantic Ocean during the past 25,000 years: Northern Hemisphere modulation of the Southern Ocean, *Earth Planet. Sci. Lett.*, *86*, 1–15, 1987.

Oppo, D. W., and S. J. Lehman, Mid-depth circulation of the subpolar North Atlantic during the Last Glacial Maximum, *Science*, *259*, 1148–1152, 1993.

Oppo, D. W., and S. J. Lehman, Suborbital timescale variability of North Atlantic Deep Water during the past 200,000 years, *Paleoceanography*, *10*, 901–910, 1995.

Rahmstorf, S., Rapid climate transitions in a coupled ocean-atmosphere model, *Nature*, *372*, 82–85, 1994.

Rahmstorf, S., Bifurcations of the Atlantic thermohaline circulation in response to changes in the hydrological cycle, *Nature*, *378*, 145–149, 1995.

Rickaby, R. E. M., and H. Elderfield, Planktonic foraminiferal Cd/Ca: Paleonutrients or paleotemperature?, *Paleoceanography*, *14*, 293–303, 1999.

Rickaby, R. E. M., M. J. Greaves, and H. Elderfield, Cd in planktonic and benthic foraminiferal shells determined by thermal ionisation mass spectrometry, *Geochim. Cosmochim. Acta*, *64*, 1229–1236, 2000.

Sarnthein, M., et al., Changes in east Atlantic deepwater circulation over the last 30,000 years: Eight time slice reconstructions, *Paleoceanography*, *9*, 209–267, 1994.

Stocker, T. F., and D. G. Wright, Rapid transitions of the ocean's deep circulation induced by changes in surface water fluxes, *Nature*, *351*, 729–732, 1991.

Toggweiler, J. R., Variation of atmospheric $CO_2$ by ventilation of the ocean's deepest water, *Paleoceanography*, *14*, 571–588, 1999.

Tziperman, E., Inherently unstable climate behavior due to weak thermohaline ocean circulation, *Nature*, *386*, 592–595, 1997.

United Nations Educational, Scientific, and Cultural Organization (UNESCO), Thermodynamics of the carbon dioxide system in seawater, *UNESCO Tech. Papers Mar. Sci.*, *51*, 1987.

Weyl, P. K., The role of the oceans in climatic change: A theory of the Ice Ages, *Meteorol. Monogr.*, *8*(30), 37–62, 1968.

Williamowski, C., and R. Zahn, Upper ocean circulation in the glacial North Atlantic from benthic foraminiferal isotope and trace element fingerprinting, *Paleoceanography*, *15*, 515–527, 2000.

Wüst, G., Schichtung und zirukulation des Atlantischen Ozeans, Die stratosphare des Atlantischen Ozeans, *Wiss. Ergebn. Dtsch. Atl. Exped. Meteor*, *6*, 109–288, 1935.

Yu, E.-F., R. Francois, and M. P. Bacon, Similar rates of modern and last-glacial ocean thermohaline circulation inferred from radiochemical data, *Nature*, *379*, 689–694, 1996.

Zahn, R., and A. Stüber, Suborbital intermediate water variability inferred from paired benthic foraminiferal Cd/Ca and $\delta^{13}C$ in the tropical west Atlantic and linking with North Atlantic climates, *Earth Planet. Sci. Lett.*, *200*, 191–205, 2002.

Zahn, R., K. Wynn, and M. Sarnthein, Benthic foraminiferal $\delta^{13}C$ and accumulation rates of organic carbon: *Uvigerina peregrina* group and *Cibicidoides wuellerstorfi*, *Paleoceanography*, *1*, 27–42, 1986.

T. M. Marchitto Jr., Lamont-Doherty Earth Observatory of Columbia University, Palisades, New York, USA.

D. W. Oppo and W. B. Curry, Woods Hole Oceanographic Institution, Woods Hole, Massachusetts, USA.